AIAA Undergraduate Design Competition: Aerial Firefighting Aircraft

A Technical Report submitted to the Department of Mechanical and Aerospace Engineering

Presented to the Faculty of the School of Engineering and Applied Science

University of Virginia • Charlottesville, Virginia

In Partial Fulfillment of the Requirements for the Degree

Bachelor of Science, School of Engineering

James Pinshi Graham

Spring, 2022

Technical Project Team Members

Spencer Barnes
Haley Knowles
Joseph Orrico
Kevin Moccia
Kobi Vance
Grace Vidlak
Brendan Whalen
Jackson Wray

On my honor as a University Student, I have neither given nor received unauthorized aid on this assignment as defined by the Honor Guidelines for Thesis-Related Assignments

Jesse Quinlan, Department of Mechanical and Aerospace Engineering

AIAA 2021-2022 Undergraduate Aerial Firefighting Aircraft

Final Design Report

Haley Knowles, Brendan Whalen, Jackson Wray, Kobi Vance, Spencer Barnes, Joseph Orrico, Grace Vidlak, James Graham, and Kevin Moccia

The Dragonforce

MAE 4660 Aircraft Design II

Department of Aerospace and Mechanical Engineering

University of Virginia, School of Engineering and Applied Science, Charlottesville, Virginia

Date of Submission: May 11ᵗʰ, 2022

Team Splashzone

Haley Knowles
Team Lead, Systems
AIAA - 1357287

Brendan Whalen
Structures, Payload
AIAA - 1342612

Jackson Wray
Structures, CAD
AIAA - 1258212

Kobi Vance
Economics
AIAA - 1357303

Spencer Barnes
Propulsion
AIAA - 1343398

Joseph Orrico
Mission Design
AIAA - 1357285

Grace Vidlak
W & B, Stability
AIAA - 1356583

James Graham
Structures, CAD & Analysis
AIAA - 1326021

Kevin Moccia
Aerodynamics
AIAA - 1344585

Faculty Advisor: Jesse Quinlan | AIAA Member #306245 | Signature:

Table of Contents

List of Figures

List of Tables

Acronyms & Nomenclature (Symbols)

ε = Error Tolerance

λ = Wing Taper Ratio

b = Wing Span

C_D = Coefficient of Drag

C_{Di} = Induced Drag Coefficient

$C_{l\beta}$ = Lateral Stability Derivative

$C_{n\beta}$ = Directional Stability Derivative

C_L = Coefficient of Lift

$C_{m\alpha}$ = Longitudinal Stability Derivative

e = Oswald Span Efficiency Factor

i_H = Horizontal Stabilizer Incidence Angle

L = Total Lift Applied to Wing

n = Load Factor

y = Distance from Root Chord

V_1 = Engine Failure Recognition Speed

V_A = Maneuvering Speed

V_B = Maximum Gust Intensity Speed

V_C = Cruising Speed

V_D = Dive Speed

V_{S1} = 1-g Stalling Speed

V_{Sneg} = Negative Load Factor Stall Speed

W_{empty} = Empty Weight

W_{fixed} = Fixed Weight

W_{fuel} = Fuel Weight

W_{TO} = Takeoff Gross Weight

AAA = Advanced Aircraft Analysis

AIAA = American Institute of Aeronautics and Astronautics

AC = Alternating Current

AGL = Above Ground Level

AOA = Angle of Attack

APU = Auxiliary Power Unit

AR = Aspect Ratio

CAD = Computer Aided Design

CAGR = Compound Annual Growth Rate

CFRP = Carbon Fiber Reinforced Polymer

CG = Center of Gravity

CONOPS = Concept of Operations

DC = Direct Current

DOC = Direct Operating Cost

DSMA = Douglas Santa Monica Airfoil

EO/IR = Electro-Optical/Infrared

FADEC = Full Authority Digital Engine Control

FAR = Federal Aviation Regulations

FLOPS = Flight Optimization System

FLIR = Forward Infrared

HUD = Head up display

LAMEA = Latin America, Middle East and Africa

LAST-II = Large Aerial Scooper Tanker II

LCC = Life Cycle Cost

MSL = Mean Sea Level

NACA = National Advisory Committee for

Aeronautics

OEI = One Engine Inoperable

OEW = Operating Empty Weight

QFD = Quality Function Development

RANS = Reynolds Averaged Navier Stokes

RDT&E = Research, Development, Test, and

Evaluation

RFP = Request for Proposal

RGF = Range Growth Factor

RTO = Rejected Takeoff

TOGW = Takeoff Gross Weight

WSR = Weight Sensitivity Ratio

3 View Drawings (Units in ft)
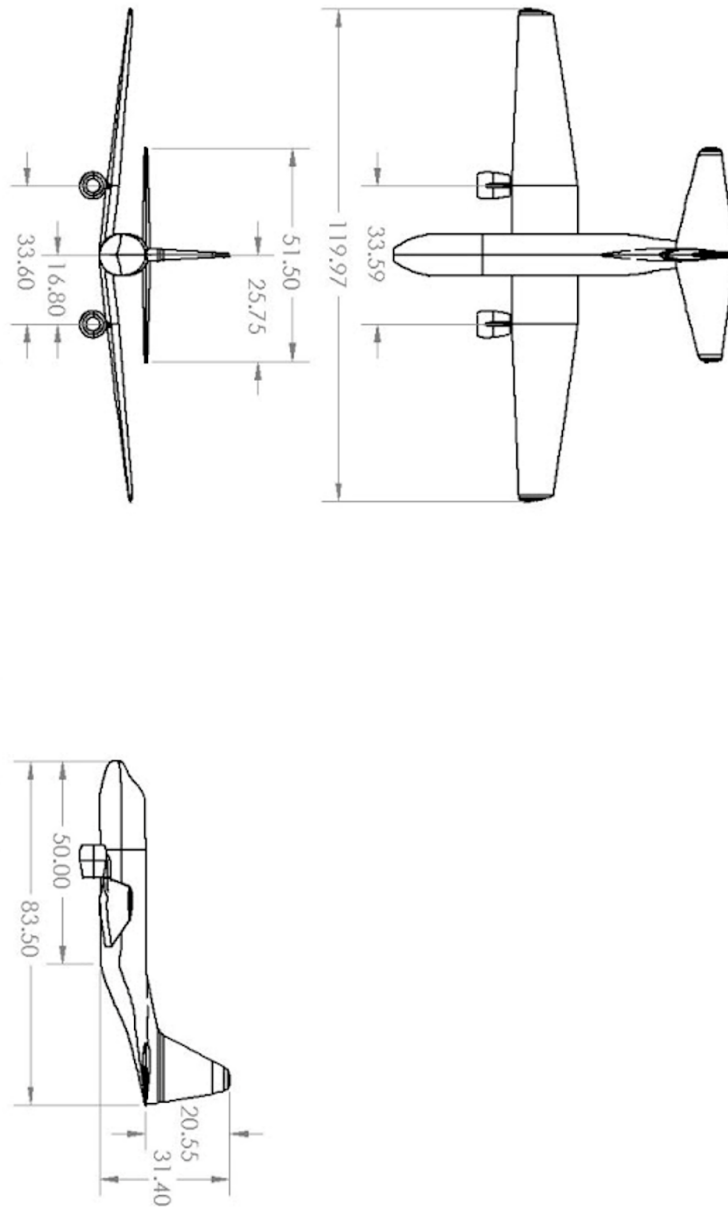
1. Executive Summary

The Splashzone aircraft design team proudly presents the Dragonforce airtanker in response to the 2022 American Institute of Aeronautics and Astronautics (AIAA) Undergraduate Team Aircraft Design Request for Proposal (RFP). This report summarizes the conceptual design of the Dragonforce, a purpose-built responsive aerial firefighting aircraft. Dragonforce eliminates the compromises and inefficiencies in the current practice of using modified airframes for aerial firefighting.

The design of the Dragonforce demonstrates a thorough understanding and evaluation of the requirements detailed by the RFP. The aircraft configuration, rendered in Figure 1-1, features a conventional tail and two CFM56-7B turbofan engines underneath a low mounted wing. Two separate internal payload tanks with a total retardant capacity of 8,000 gallons meet the RFP objective, and a computer-controlled gravity-fed dispersal system enables multiple-drop capabilities of at least 2,000 gallons. Dragonforce has a take off gross weight (TOGW) and operating empty weight (OEW) of 181,800 lbs and 93,600 lbs, respectively. As specified by the RFP, the aircraft is designed for a design mission radius with full payload of 400 nautical miles and a ferry mission range of 2,000 nautical miles. Existing systems have been used in the design where possible, minimizing associated costs and ensuring entry into service by 2030.

Figure 1-1. Dragonforce Aircraft

2. Introduction

Continued changes to the planet's climate have increased the number and intensity of wildfires, posing ever greater threats to life and property. Historically, major aerial firefighting platforms consist of modified military or commercial airframes with internal or external equipment integrated into the original designs and structures, such as variants of the Lockheed Martin C-130 Hercules and Boeing's 747 aircraft (AIAA, 2021). Dragonforce allows responsible organizations the ability to fight wildfires more efficiently from the standpoint of both performance and cost.

The design process began with careful review of the aerial firefighting market and RFP requirements and objectives. Initial aircraft sizing, including weight estimation, was performed using custom MATLAB scripts, and NASA's Flight Optimization Software (FLOPS) was used to perform mission analysis. Aerodynamic performance was assessed using NASA's VSPAERO and DARcorporation's FlightStream, and the propulsion system performance was modeled using GasTurb. Modeling of the conceptual designs and finite element structural simulations were performed in SolidWorks. Additionally, cost estimations were made using the Advanced Aircraft Analysis (AAA) software. The design process was highly iterative, and design cycles were repeated until the team converged on a final design for Dragonforce that best satisfied the requirements and objectives in the RFP. The remainder of this report encompasses detailed design information and outlines the conceptual design process behind the Dragonforce.

3. **Market Analysis**

This section is focused on the overall aerial firefighting market. The section is intended to be a useful introduction to the scope of the project and the motivation to the project in general. Furthermore, the section lists key players involved in all aspects of aerial firefighting operations, including end-users and manufacturers. When developing a new product, it's extremely important to know how it will penetrate the existing market and complement current aerial firefighting platforms. This section aims to characterize the current aerial firefighting market.

3.1 Stakeholder List

The following list has been developed to identify any possible stakeholders—parties with an interest or concern in the design process as a whole.

- **American Institute of Aeronautics and Astronautics:** As the entity responsible for the design competition, the AIAA remains an important stakeholder and source for design guidelines.

- **Manufacturers:** The design will utilize many pre-existing technologies, so manufacturers will play an important role. The manufacturing process may be divided into multiple producers, which may lead to the consideration of third party manufacturers to acquire parts.

- **End-user:** Airtanker pilots and air tactical supervisors are the main end-users for the aircraft. These users value the ability to complete the mission quickly and effectively without sacrificing safety. The team also considered the ability for these end-users to perform multiple roles with ease and convenience during the mission.

- **Firefighting Organizations and Military:** There are two service provider segments for all firefighting aircraft worldwide. Specifically in North America, CAL Fire and the United States Forest Service are two major fire fighting organizations, and they operate under the United States Government and Department of Defense. The utilization of preexisting technology from military aircraft and their continued involvement in firefighting aviation deems the military a main stakeholder as well.

3.2 Market Size

The global firefighting aircraft market was valued at $8.85 billion in 2020 and is projected to reach $16.47 billion by 2030. This upward shift would register a compound annual growth rate (CAGR) of 6.5% from 2021 to 2030 (Allied Market Research, 2021). Although the global economy suffered a major blow due to the COVID-19 pandemic, the spending on firefighting equipment did not decline in 2020 and 2021. Some of the largest bushfire occurrences in the recent past prompted the governments to enhance their aerial firefighting capabilities. Hence, an opportunity to develop state-of-the-art wildfire fighting aircraft exists.
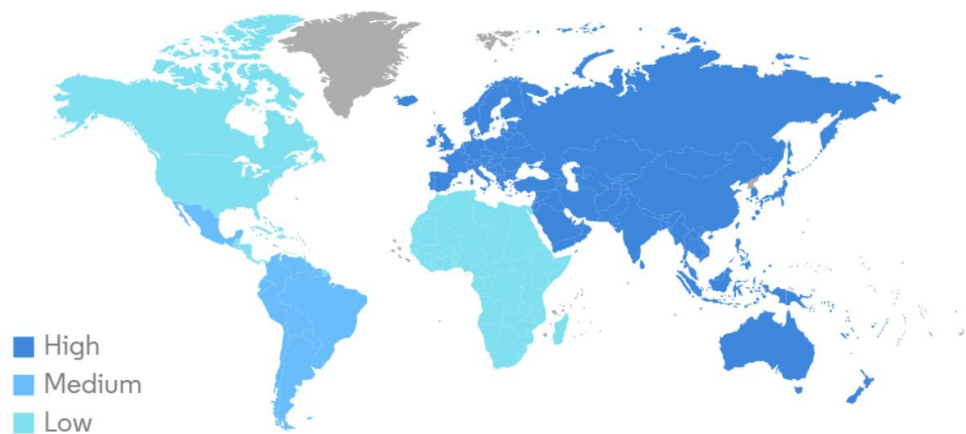
Figure 3-1. Firefighting Aircraft Market: Growth Rate by Region (2022-2027)

During the forecasted period of about 5 years from now, Asia-Pacific areas are expected to experience the highest growth in the aerial firefighting market. The prevalent practice of slash and burn agriculture, combined with the extreme effects of El Nino and La Nina events, intensified the hazard of forest fires in the Asia-Pacific region (Helan, 2022). The growing instances of wildfires and the resulting extensive damage have encouraged regional fire protection authorities to expand their firefighting aircraft fleet.

3.3 Competition

The market of firefighting aircraft is highly concentrated as only a few players are involved: Lockheed Martin Corporation, ShinMaywa Industries Ltd, Textron Inc., Leonardo SpA, and Airbus SE. Together, these major market players account for a significant share of the total market due to their strong order book and deliveries to

firefighting agencies worldwide. These companies are looking to invest in the development of new aircraft models for firefighting that emphasize the capability to carry and drop massive volumes of water and fire retardant.

3.4 Segment Analysis

The global freighting aircraft market is segmented by type, service provider, max takeoff weight, water capacity, and region. By type, the market is segmented into fixed wing and multi-rotor. By service provider, it is segmented into firefighting organizations and the military. By max takeoff weight, the global market has segmented into below 110,000 lbs and above 110,000 lbs. By water capacity, it is segmented into less than 5,000 gallons, 5,000 to 10,000 gallons, and more than 10,000 gallons. By region, the global market is spread across North America, Europe, Asia Pacific, and LAMEA.

Specifically examining the fixed wing and multi-rotor segments, the latter accounted for the largest market share in 2021. Although helicopters can carry less fire retardant and water than fixed-wing aircraft, they can be used to transport firefighters and deploy equipment rapidly. Helicopters are useful for fast initial attacks on smaller wildfires; the operational benefits of using rotorcraft for freighting missions have led to a steady increase in demand for firefighting rotorcraft on a global scale. Furthermore, the demand for helicopter conversions for firefighting increased, and several players are converting existing helicopter models into firefighters with the integration of modern internal tanks and other equipment. Based on this market assessment, it's clear that a clean-sheet very large air tanker class firefighting aircraft is needed and would fill gaps in the global market.
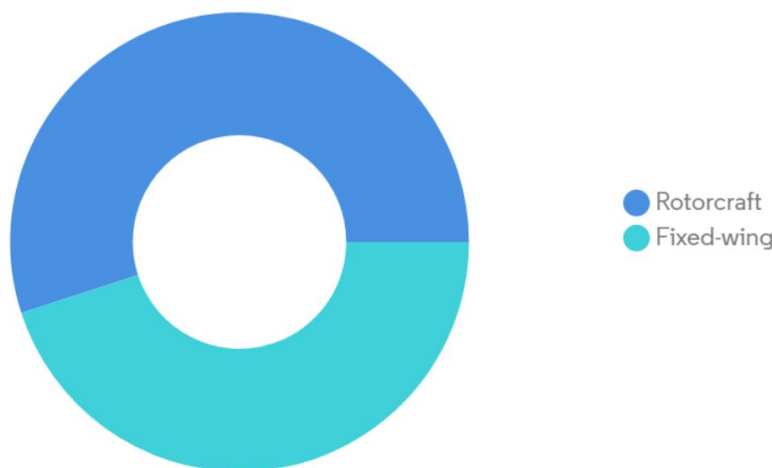
Figure 3-2. Firefighting Aircraft Market: Revenue (%), by Aircraft Type, Global 2021

4. Concept of Operations, Requirements, and Mission Profile

In this section, the characteristics of the proposed system are described. The requirements subsection outlines the basic capabilities of the aircraft in terms of general requirements, design mission requirements, and firefighting mission requirements. Next, the CONOPS and Mission Profile Sections detail the team's vision for operation and important mission characteristics. The design must not only meet the AIAA requirements, but must also comply with any specifications, standards, and regulations put forth by the governing bodies in the area of operation.

4.1 Requirements

The RFP provides several general requirements and objectives that must be met by the conceptual design (Table 4-1). Requirements must be met; whereas, objectives are optional goals. The Dragonforce met all of the requirements put forth in the RFP.

Table 4-1. RFP General Requirements

Requirement	Comments
The airplane design shall meet applicable certification rules in FAA 14 CFR Part 25.	Required
The airplane shall be capable of flight in known icing conditions.	Required
The airplane shall be capable of VFR and IFR flight with an autopilot.	Required
The balanced field length of the airplane design shall be less than or equal to 8,000 ft at 5,000 ft MSL elevation on a +35°F hot day.	Required
The balanced field length of the airplane design shall be less than or equal to 5,000 ft at 5,000 ft MSL elevation on a +35°F hot day.	Objective or Goal
The airplane shall have a minimum ferry range of 2,000 n mi with no payload.	Required
The airplane shall have a minimum ferry range of 3,000 n mi with no payload.	Objective or Goal
The airplane shall have a minimum dash speed of 300 kts after payload drop.	Required
The airplane shall have a minimum dash speed of 400 kts after payload drop.	Objective or Goal
The airplane design, assuming reserves and equipment required to meet applicable FARs, shall provide systems and avionics architecture that will enable autonomous operation; this includes the providing of a market justification for choosing to either provide or omit this capability and a determination of how the design would change with this capability.	Objective or Goal

In addition to general requirements, the RFP provides design mission requirements (Table 4-2). These include an entry into service before 2030 and multi-drop capability. Similar to the general requirements, the Dragonforce meets all specifications.

Table 4-2. Design Mission Requirements

Requirement	Comments
The mission shall have an Entry Into Service date of no later than the year 2030.	Required
The airplane shall use existing engine(s) or one that is in development to be in service by the year 2028, or at least two years prior to the airplane EIS.	Required
The assumptions on at least specific fuel consumption/efficiency, thrust/power and weight shall be documented.	Required
The airplane shall be multi-drop capable. With a minimum of 2,000 gallons/drop.	Required
The airplane shall have a minimum radius of 200 n mi with full payload.	Required
The airplane shall have a minimum radius of 400 n mi with full payload.	Objective or Goal

Finally, the RFP provides firefighting mission requirements (Table 4-3). These include a minimum fire retardant capacity of 4,000 gallons and a retardant density of at least 9 lbs/gal. The Dragonforce meets all of the requirements below.

Table 4-3. Firefighting Mission Requirements

Requirement	Comments
The airplane shall have a minimum fire retardant capacity of 4,000 total gallons.	Required
The airplane shall have a minimum fire retardant capacity of 8,000 total gallons.	Objective or Goal
The fire retardant reload shall be greater than or equal to 500 gal/min.	Required
The fire retardant shall have a density of at least 9 lbs/gal.	Required
The airplane shall have a payload drop speed of less than or equal to 150 kts.	Required
The airplane shall have a payload drop speed of less than or equal to 125 kts.	Objective or Goal
The drop altitude shall be less than or equal to 300 feet above ground level	Required

4.2 Concept of Operations

The primary requirements listed previously state that an aircraft will be designed with the sole purpose of fighting wildfires, as the majority of aircraft currently in service for firefighting purposes are modified commercial or military planes. The purpose-built design should ideally trade robust structural designs with easily repairable/replaceable structures for optimal weight savings.

Key design objectives include minimizing operation and support costs using modularity, facilitating rapid repairs and replacements, and ensuring reliability. The production cost of the aircraft should be minimized by choosing materials and manufacturing methods appropriate for the annual production rate. The aircraft's reliability, maintenance (failure rate, time-to-repair, etc), and operational availability should be equal or better than that of comparable aircraft as well.

Considering these requirements as listed by the Request for Proposal, the following mission profile corresponding with the final design was developed. Maximizing the fire retardant capacity was a priority for the design. The 8,000 gallon retardant capacity objective was a centerpiece of the design, and many design decisions were made to ensure this objective was met.

4.3 Mission Profile

The Dragonforce has a design mission profile as shown below in Figure 4-1. The profile begins with takeoff and a climb up to cruise altitude. The climb is followed by a cruise segment that represents the need for the aircraft to arrive at the location of the fire. After reaching this location, the mission is followed by three sets of retardant drops, each separated by a loiter segment—representing the potential need for the aircraft to wait a given amount of time before the next drop or the need to travel to a different location. Due to the RFP requirement of a drop altitude less than or equal to 300 ft AGL, this requires a descent and climb (steps 4 and 10) surrounding the drop portion of the mission. Finally, the mission ends with a return cruise segment and a descent and land.
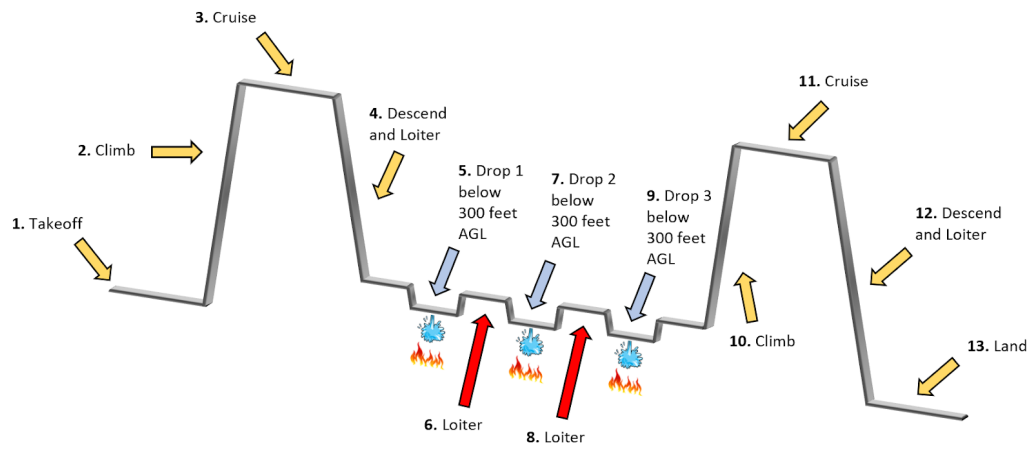
Figure 4-1. Design Mission Profile

5.   **Configuration and Payload Capabilities**

This section begins by providing a high level summary of the major configuration choices made by the team and how the RFP requirements influenced these design choices. Emphasis is placed on the retardant payload requirement as that was a major driving force in the design of the Dragonforce. Next, the external configuration of the fuselage, wing, and empennage is discussed in detail including the reasoning for the chosen configurations. The next subsection describes the chosen payload configuration to hold the fire retardant in addition to the justification for its design and the associated weight estimations. Finally, the internal layout of the aircraft fuselage and sub-systems is presented.

5.1 Design Morphology

The RFP required 4,000 gallons of retardant payload and stated an objective capacity of 8,000 gallons. This range of payload volumes represents a range in payload weight of 36,000 lbs to 72,000 lbs and thus represents a key consideration for the design and structure of the aircraft. Based on the market analysis early in the design process, the decision was made to meet the objective of carrying 8,000 gallons of retardant. Designing to meet this objective had extensive implications for the overall configuration of the aircraft. Emphasis was additionally placed on minimizing the cost of manufacturing and operating the aircraft. Novel aircraft configurations were initially considered, but the design quickly converged to a conventional configuration. Such a configuration enables modularity in the design and has safety and performance that is well established, which enables significant reductions in the development cost.

Fundamentally, the high weight and high density of the payload drove the design towards a large wing and small fuselage configuration. While minimizing the fuselage size for the operator's cabin and payload, consideration was given to ensuring a sufficient moment arm of the tail to provide proper stability and control of the aircraft. Various analyses were performed as the tail was iteratively sized and refined to ensure stability of the aircraft while minimizing the aircraft's overall size. While an entirely integrated payload tank was initially considered, the final design prevents the structural airframe components from coming into direct contact with the corrosive fire retardant. The tank dimensions were defined to minimize the overall size of the fuselage while ensuring it was long enough to maintain the aircraft stability and meet the capacity objective.

5.2 External Configuration

The final Dragonforce design configuration was optimized to carry the objective payload amount while meeting the performance requirements set out in the RFP. Dragonforce is a conventionally configured tube and wing aircraft design. A low mounted wing with a relatively large wing surface area of 1,592 ft^2 was selected to ensure sufficient lift and stability of the aircraft during flight operations. The high density of the payload and the low drop speed requirement of less than 150 kts drove the selection of a large wing for the Dragonforce. A large conventional tail is configured to provide proper stability and control of the relatively compact fuselage. The very large air tanker is powered by two CFM56-7B turbofan engines that are forward mounted on pylons under the wings. The wing and engine configuration ensures high lift capabilities at the low speeds required for an accurate payload drop and also sufficient thrust for the dash speed following dispersal. Tricycle-style landing gear that retracts into the fuselage during flight was selected for the Dragonforce. With these major configuration aspects, the aircraft is designed to be compact, efficient, and cost effective to both manufacture and operate.
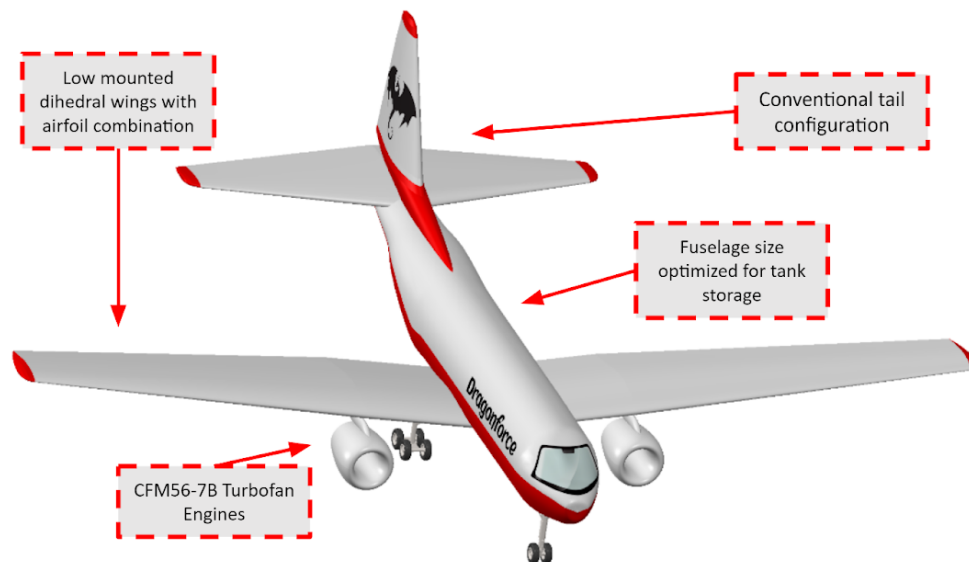
Figure 5-1. General Configuration Diagram of the Dragonforce

5.3 Payload Capabilities

The trapezoidal tank geometry with a capacity of 4,000 gallons is shown in Figure 5-2. Two of these tanks are integrated into the aircraft fuselage to provide the objective capacity of 8,000 gallons. A lower hopper made of stainless steel is integrated into the fuselage floor and connected to the replaceable upper tank portion made of

lightweight polyethylene above the fuselage floor. Hydraulically operated aluminum firegates serve as the interface of the retardant payload and surrounding atmosphere. A baffling system is implemented in the tank interior to minimize the sloshing effect that arises from a liquid payload and affects aircraft dynamics. The baffling system, also shown in Figure 5-2, features four evenly spaced cross-sectional panels with perforations that allow retardant to flow between the individual compartments. This system minimizes the effects of rolling and pitching moments that result from shifts in the center of gravity.
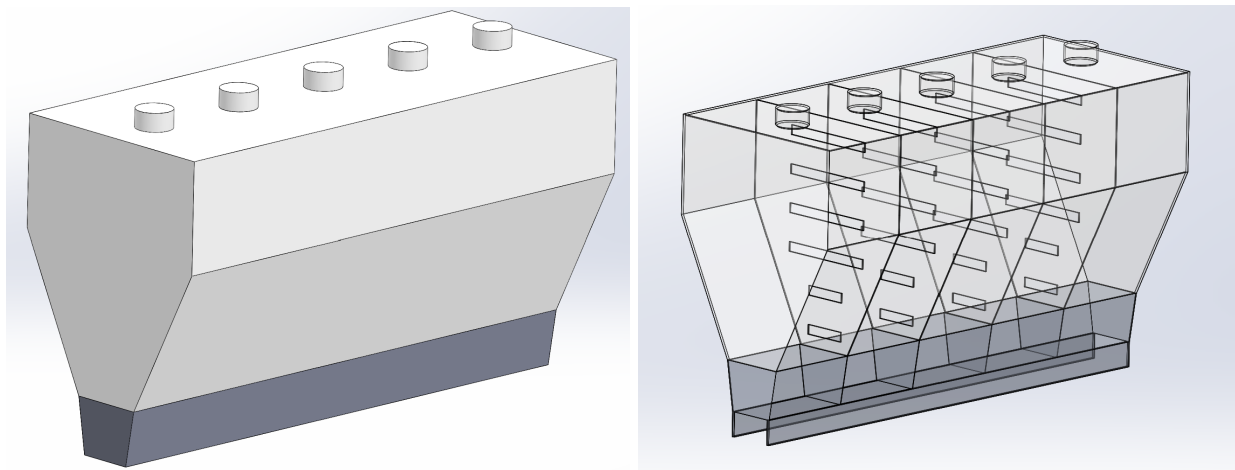
Figure 5-2. Tank Geometry and Baffling System

Since the tank is gravity-fed, the trapezoidal design will not have the additional stresses of a pressurized system, and the selected thickness of each material section is enough to handle the hydrostatic pressure and dynamic loads that the retardant payload places on the tank. The trapezoidal structures of the lower hopper and upper tank are also more cost effective to manufacture than more complex shapes. The materials and weight estimations of the individual tank components are shown in Table 5-1.

Table 5-1. Tank Materials, Weights, and Volumes

Component	Material	Weight (lb)	Volume (gal)
Upper Tank	Polyethylene	960	3810
Hopper	SS 304	420	300
Firegates	Al 7075	660	N/A
	Totals	**2,040**	**4,110**

A GPS-linked computer-controlled dispersal system was selected to control the fire gates and deliver the desired flow rate of retardant to the target area. Hydraulic actuators control the firegates. The use of a GPS linked system allows for accurate delivery to the target area and for the flow rate to be based on the aircraft ground speed. Based on preliminary flow rate calculations, the system is capable of releasing the full load in less than seven seconds. Gravity-fed dispersal, as opposed to a pressurized system, eliminates the need for auxiliary pressurization systems and minimizes the structural strength requirements of the tank while still maintaining the desired flow rate and coverage levels. The system provides the Dragonforce operators with real-time flow rate adjustment technology, resulting in superior drop zone coverage and accuracy.

5.4 Internal Layout

The guiding objective for the internal layout is to efficiently utilize the entirety of the fuselage volume. This not only reduces the structural weight of the aircraft, but enables more efficient operation in terms of reducing drag and increasing maneuverability. Such a layout eliminates the unnecessary empty space that is common in aircraft retrofitted for air tanker operations. While the total fuselage length is 83.5 feet, the usable fuselage length of 50 feet is defined by the area forward of the tail section. This length is split into the 15 foot cockpit and 35 foot main fuselage compartments, with a structural bulkhead separating the two. The remaining fuselage length beyond the payload tanks encompasses the volume below the tail section. This volume is reserved for auxiliary systems and additionally encompasses the location of the cargo bay door, which gives easy access to the interior of the fuselage for maintenance and inspection.
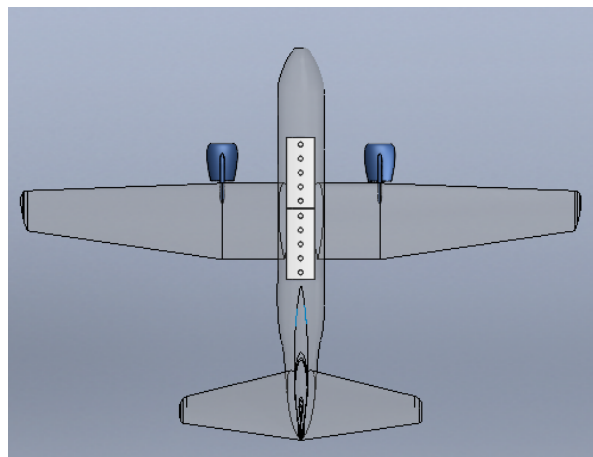
Figure 5-3. Location and Relative Size of Retardant Tanks in the Fuselage

The two tanks are centered around the CG of the aircraft, and the retardant dispersal is synchronized to minimize CG shifts during the dropping operation. Two feet of space is left on either side of the payload to allow the operator ample room to walk beside the tanks and perform inspections or maintenance as shown in Figure 5-4.
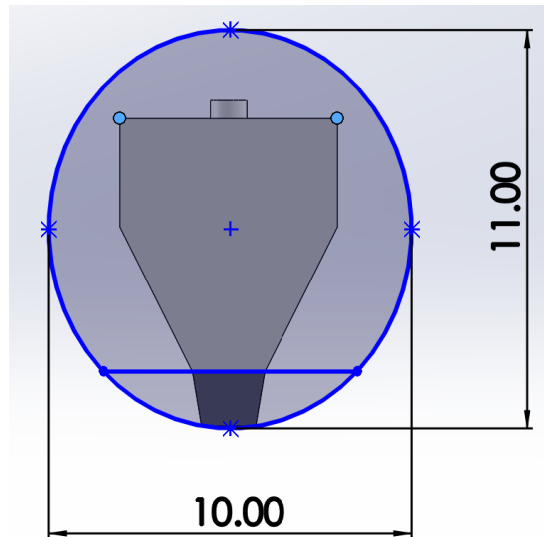
Figure 5-4. Dragonforce Fuselage Dimensions with Cargo Floor and Payload Tank (Units in ft)

6.   Downselection to Final Design and Tradeoff Analysis

The design cycle began through a concept ideation process where every team member analyzed the requirements and objectives of the challenge and created an individual basic aircraft configuration. The team then decided to choose three aircraft configurations to advance before rigorously downselecting to a final design. The initial three configurations each possessed unique features which were identified as factors that would influence meaningful trade studies. These differing factors included payload capacity, wing and tail configuration, engine choice, and mission profile. Following the generation of each configuration, an initial design cycle was completed for each of the three configurations in order to gain insight into areas such as weight, performance, and cost to effectively complete the downselect process to a final design.

6.1 Preliminary Configurations

The three preliminary configurations were the initial Dragonforce, the Zeus-8k, and the Large Aerial Scooper Tanker II (LAST II).

The initial Dragonforce (see Figure 6-1) is a modification of the Lockheed Martin C-130 Hercules. The three major modifications from the original airplane are a low wing placement, turbofan engines, and an extended fuselage. These modifications were enacted to fulfill the balanced field length and payload capacity requirements. The initial Dragonforce is intended to carry approximately 8,000 gallons of fire retardant and follow the mission profile as seen in Figure 6-1.
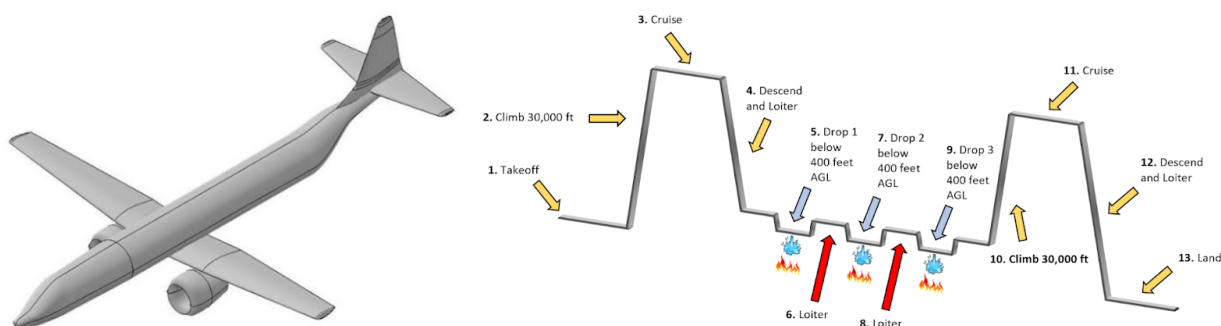
Figure 6-1. Initial Dragonforce Configuration and Mission Profile

The Zeus-8k (see Figure 6-2) is an adaptation of the DC-10 airtanker. The goal of this design was to create a lighter and more maneuverable version of the DC-10 with a higher lift capability and a larger propulsion system. The dimensions were downsized from the original aircraft to account for the reduction in payload capacity, and two additional modifications were the implementation of four turboprop engines and a T-tail configuration. Zeus-8k is intended to carry approximately 8,000 gallons of fire retardant and follow the mission profile as seen in Figure 6-2.
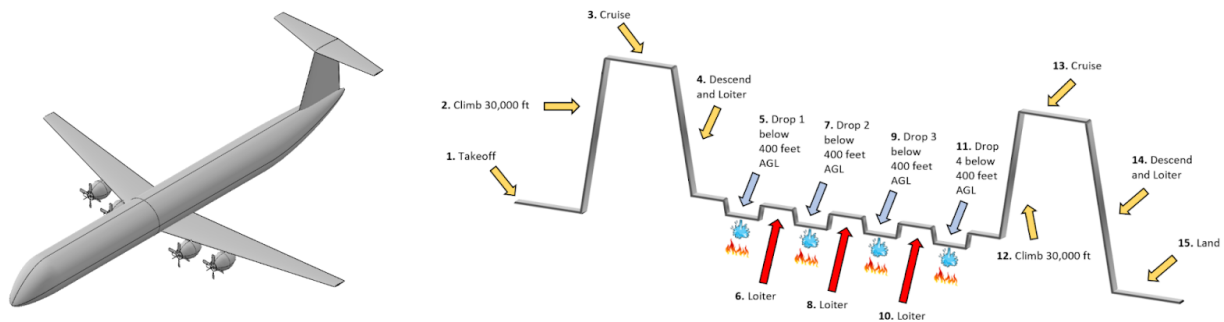
Figure 6-2. Zeus-8k Configuration and Mission Profile

The LAST II (see Figure 6-3) is another adapted C-130 with modifications for amphibious operation and scooping capabilities. Fundamental changes include the addition of a flying boat hull based on the design of the CL-415, replacement of the conventional tail with a cruciform, and removal of the mid-wing span fuel tanks in favor of floats placed at the wing tips. The design dimensions are slightly larger than the C-130 given the additional payload capacity. LAST II is intended to carry approximately 4,000 gallons of fire retardant and follow the mission profile as seen in Figure 6-3.
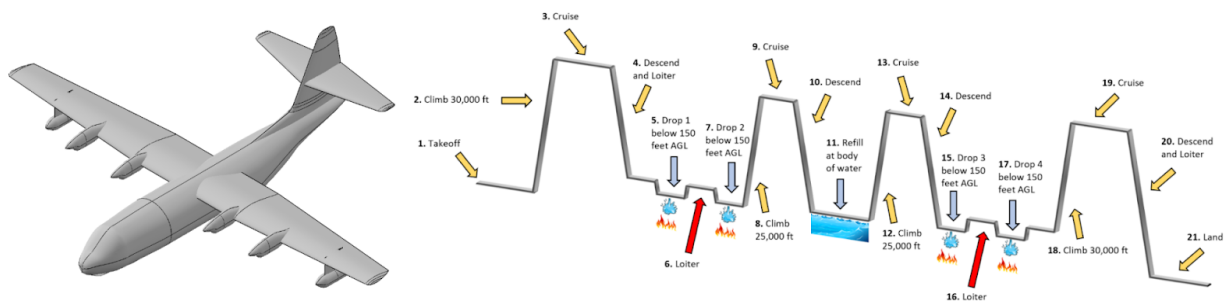
Figure 6-3. LAST-II Configuration and Mission Profile

6.2 Configuration Downselection

After the three configurations were chosen, an initial design cycle was conducted for each aircraft in order to refine each configuration and determine key parameters that would aid in the downselect process. The general design and analysis approach was first to run several aerodynamic simulations using VSPAERO software to conduct preliminary stability analyses. This software was chosen as a first pass due to the ease of running the simulation, since all aircraft configurations were modeled using the openVSP software. Control surfaces were added to the wing and tail to examine takeoff and landing conditions. Propulsion and landing gear systems were chosen based off of comparator aircraft, and the fire retardant tanks were designed to accommodate the payload specifications. To develop a weights estimation and analyze mission performance, NASA's Flight Optimization System Software was utilized (NASA, 2020). FLOPS models were developed for each aircraft and used to estimate preliminary weight and mission performance properties such as TOGW and block fuel burn. Finally, cost analysis was conducted using AAA software, with inputs determined through FLOPS output and assumptions based on Jan Roskam's (1985) textbook, *Airplane Design*.

The key parameters for each configuration are tabulated below in Table 6-1. As can be seen from comparing the values in the chart, the Dragonforce was found to be the favorable configuration. The Dragonforce is the lightest, most fuel efficient, and least costly of the three configurations, and for this reason it was selected as the aircraft to move forward with through the design process. It should be noted that the other unique features of the Zeus-8k and the LAST-II, such as wing and tail configuration, would still be considered in trade studies to ensure an optimal choice for the final design. However, the design would be iterated upon starting with the current Dragonforce configuration. The following section will cover the sizing process utilized to finalize the aircraft configuration.

Table 6-1. Key Parameter Comparison Between Initial Configurations

	Dragonforce	Zeus-8k	LAST-II
TOGW (lbs)	273,386	327,990	452,380
Block Fuel Burn (lbs)	41,794	64,770	164,947
Wing Area (ft^2)	1,758	1,498	1758
C_L (Cruise)	0.5843	0.7558	0.6837
Field Length (ft)	7,000	7,000	7,000
Engine Weight (lbs)	10,514	16,756	6,560
TSFC	0.627	0.37	0.46
Operating Cost (USD per Hour)	3,779	4,280	6,284
Life Cycle Cost (Bil. of USD)	5.41	6.59	7.34

7. Sizing Analysis

This section of the report describes the initial sizing and constraint analysis conducted by the team in order to investigate the feasible design space and the corresponding optimal design region for the final design. The initial sizing analysis was completed through a TOGW estimation, and the constraint analysis was completed through the generation of a matching plot. Finally, the general sizing methodology explaining how the team arrived at the final Dragonforce configuration is discussed.

7.1 Initial Sizing Analysis

In order to begin the design process, TOGW provides a primary estimate of the overall aircraft size. TOGW was estimated for the initial Dragonforce configuration using an algorithm presented by Leland Nicolai and Grant Carichner in their textbook, *Fundamentals of Aircraft and Airship Design* (Nicolai & Carichner, 2010). The algorithm follows the steps below, where TOGW or W_{TO} is defined as the total weight required to perform the mission, W_{fuel} is defined as total fuel weight required to perform the mission, W_{fixed} is defined as the payload including anything that can be removed from the aircraft while still being able to fly, and W_{empty} is defined as the structure, propulsion, subsystems, etc.

1. Pick a W_{TO}

2. Compute W_{fixed} based on design mission, crew, payload, etc.

3. Estimate W_{fuel} using segment fuel fractions based on mission design

4. Compute $W_{empty,avail}$ as $W_{empty,avail} = W_{TO} - W_{fuel} - W_{fixed}$

5. Compute $W_{empty,req}$ using historical data or trends

6. Compute $W_{empty,avail} - W_{empty,req}$

7. Iterate on W_{TO} until $(W_{TO})_{new} - (W_{TO})_{old} < \varepsilon$

The algorithm was coded in MATLAB with an error tolerance (ε) of 1×10^{-6} and three graphs were generated: (1) Available and Required Empty Weight versus Takeoff Weight, (2) Takeoff Weight versus Fixed Weight, and (3) Takeoff Weight versus Range. The Available and Required Empty Weight versus Takeoff Weight graph for the initial Dragonforce configuration was utilized to find the TOGW, where the intersection of the two lines provides this value as shown below in Figure 7-1.
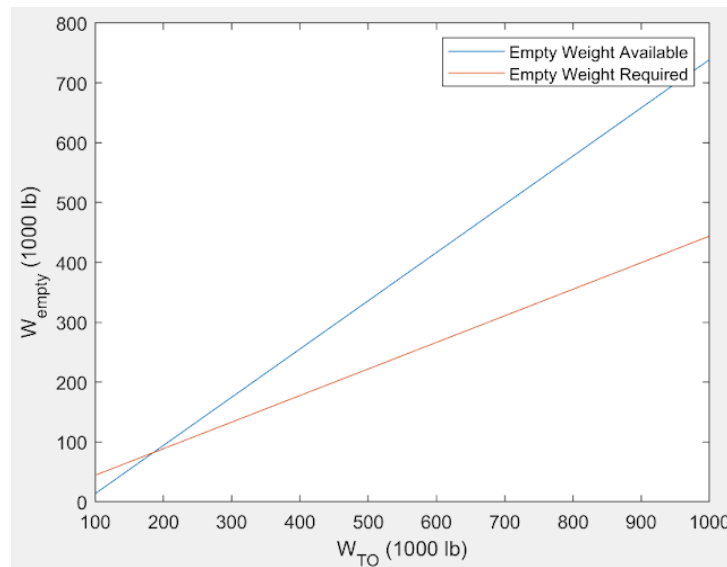
Figure 7-1. Available and Required Empty Weight versus Takeoff Weight for the Initial Dragonforce Configuration

Additionally, the weight sensitivity ratio (WSR) and range growth factor (RGF) were calculated through the generation of the other two graphs. The WSR is the slope of the Takeoff Weight versus Fixed Weight graph and is a measure of how much the TOGW is influenced by payload. The RGF is the slope of the Takeoff Weight versus Range graph and is a measure of how much the TOGW is influenced by range. The TOGW, WSR, and RGF values are summarized below in Table 7-1.

Table 7-1. Tabulated TOGW, WSR, RGF Values for the Initial Dragonforce Configuration

	Dragonforce
TOGW (lbs)	185,170
WSR	2.76
RGF (lbs/nmi)	57.2

7.2 Initial Constraint Analysis

After completing the TOGW estimation, the team generated a matching plot. Matching plots are visual depictions of the feasibility of design spaces shown in wing loading (W/S) versus thrust loading (T/W) space. Performance requirements and constraints were identified, and functional forms of these constraints were developed using W/S and T/W terms. Research was then conducted to choose reasonable values for each of the parameters in the equations, and the assumptions and justifications for these decisions are provided. These equations were then

plotted in W/S versus T/W space for each of the aircraft configurations, and the regions representing the optimal design spaces were identified.

The six constraint curves plotted were stall speed, takeoff distance, landing distance, cruise speed, rate of climb, and sustained load factor (2 equations). After these curves were plotted, the desirable sides of the curves were identified, which are represented by the arrows in the figure below. Finally, the plot was analyzed to determine the feasible design space, which is denoted by the striped region.
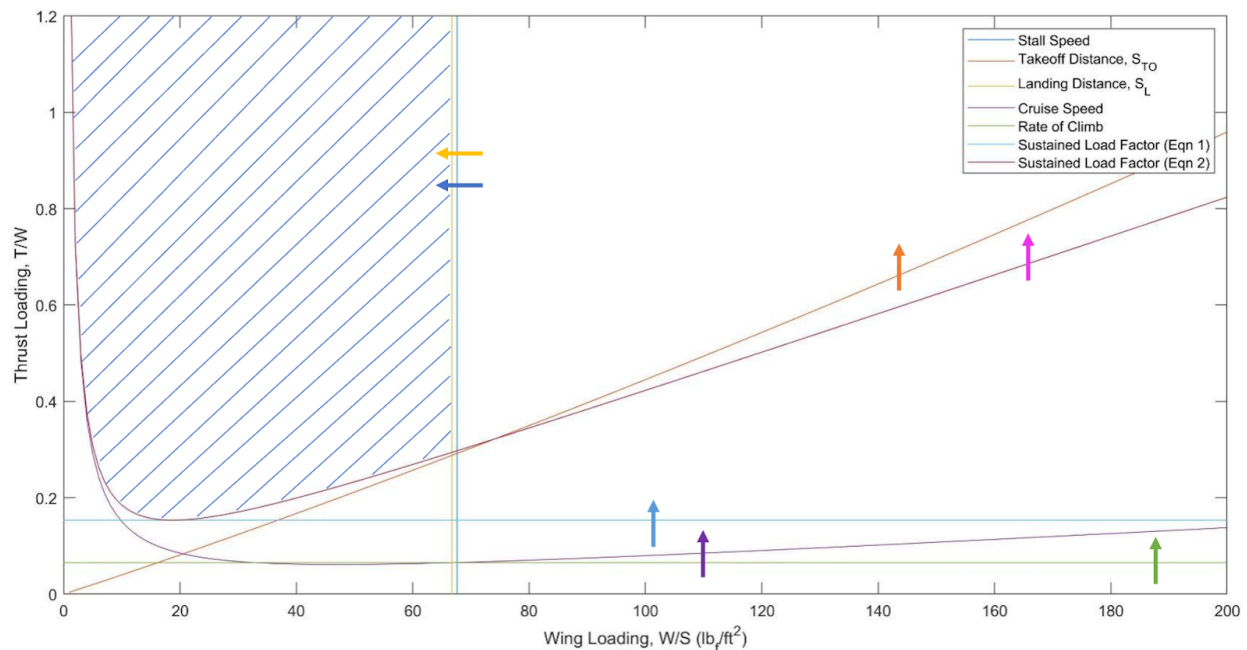
Figure 7-2. Wing Loading versus Thrust Loading Ratio for the Initial Dragonforce Configuration

Our analysis indicated a feasible design region of less than about 70 lb_f/ft^2 in wing loading and upwards of 0.15 in thrust loading. This wing loading range is comparable to utility transport aircraft like the C-130, which typically have a wing loading value between 40 - 90 lb_f/ft^2.

7.3 Sizing Methodology

After the TOGW estimation and matching plot constraint analysis, the initial Dragonforce configuration was run through the FLOPS model, as mentioned previously in Section 6.2. The output of this model gave a gross weight estimation of 273,386 lbs, which was much greater than the initial TOGW estimation of 185,170 lbs. This can be explained by the higher fidelity weight approximation methods through FLOPS with refined estimations.

Following this analysis, the goal for the sizing method was to minimize the weight of the aircraft. The main constraints that conflicted with this goal were the retardant payload (and resulting tank size) and the tail size, as a shorter fuselage results in a larger empennage. The fuselage design space provided the most variability, as the investigation of fuselage length ranged from a value of 50 to 170 feet. The upper limit comes from the initial Dragonforce configuration, and the lower limit was deemed to be the minimum value due to the total tank length of 30 feet and need for additional room for the cockpit and additional storage space. This design space is shown below in Figure 7-3, where the extra unused space can be seen in the leftmost image.
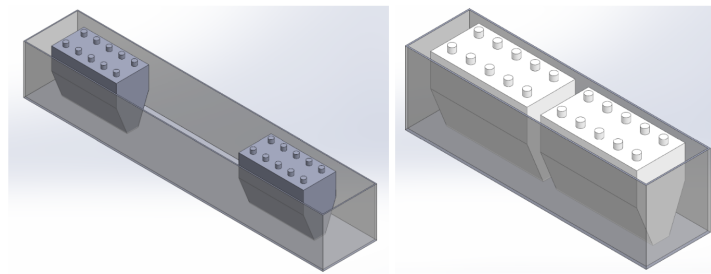
Figure 7-3. Tank Size and Resulting Fuselage Design Space

Additionally, as discussed in Section 5.5, the height and width of the fuselage were constrained by the tank size. Consequently, the tanks were designed to be longer so that the height and width of the fuselage could be minimized in order to minimize the weight of the fuselage and the drag of the aircraft. Multiple iterations of fuselage length and resulting tail size were configured and aerodynamically tested, and the optimal design was found to utilize a fuselage length on the shorter end of the design space, with a value of 83.5 feet. This design minimizes the fuselage length while still allowing enough space for the retardant tanks and without allowing the tail size to grow too large—resulting in added weight and significant drag. This methodology resulted in a 33.5% decrease in gross weight, from an initial gross weight of 273,386 lbs to a final weight of 181,805 lbs.

8.   Propulsion

Propulsion is integral to any aircraft as it provides thrust, one of the four major aircraft forces. This section details the selection and performance of the engine using three subsections: engine selection, engine performance, and airframe integration. The Engine Selection Section compares different engine types and justifies one that could realistically satisfy the design requirements. Additionally, this section details the down-selection process until only one engine is left. Next, the Engine Performance Section details all of the relevant engine metrics. Finally, the Airframe Integration Section examines the placement of the engine within the larger design.

8.1 Engine Selection

Aircraft engines can be broadly classified into six categories: piston-prop, turboprop, turbofan, turbojet, afterburning turbojet, ramjet, and rocket. Figure 8-1 below shows the operating envelope for each class of engine. Based on the objective dash speed and comparator aircraft, the team decided to aim for a true airspeed of 400 kts and an altitude of 20,000 ft. From the figure, this design requirement can be met using any of the engines except the piston-prop, eliminating it from consideration. Moreover, turbojets, afterburning turbojets, ramjets, and rockets were removed from consideration because they significantly exceeded the mission requirements, leaving turboprop and turbofan engines as the two remaining candidates.
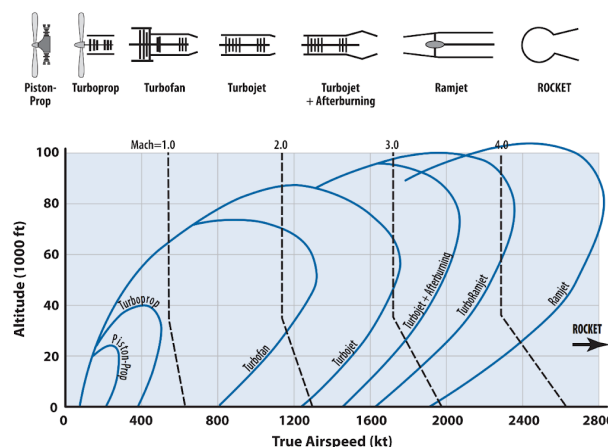
Figure 8-1. Altitude versus True Airspeed Performance Regimes for Different Engine Types

Turboprop and turbofan engines are quite similar, with the primary difference being a large ducted fan on the front of the turbofan. While turboprops are more efficient, turbofans can produce more thrust and operate at

higher altitudes. Since the operating envelope of turboprops at low altitudes ends at airspeeds of 400 kts, the team decided to use turbofan engines to ensure sufficient thrust.

After choosing a turbofan engine, the team compared three engines from different U.S. manufacturers: CFM56-7B, V2531-E5, and Trent 500 (Table 8-1). These three engines were chosen because they were used on comparator aircraft with a similar TOGW to the Dragonforce. While the Trent 500 has more thrust than the other two engines, it also weighs significantly more and has a lower thrust to weight ratio (EASA, 2021). Additionally, the team discerned that the thrust rating was significantly higher than necessary for the Dragonforce. Based on these factors, the Trent 500 was removed from consideration. Between the CFM56-7B and the V2531-E5, the latter has a higher thrust, weight, and thrust-to-weight ratio (EASA, 2019). On the other hand, the CFM56-7B has a higher bypass ratio, which is typically indicative of a higher efficiency (Balle, 2020). Furthermore, Table 8-1 does not consider the "-illities," such as manufacturability, reliability, and affordability. The CFM56 is the best selling jet engine in history, with over 900 million flight-hours (CFM, 2018). Because it has a proven track record, the team surmised that it would perform better on the "-illities" that are difficult to quantify in early design and thus be a better candidate, especially considering the similar performance of the two engines.

Table 8-1. Comparison of Relevant Engine Characteristics for Three Prospective Engines

Engine Characteristic	CFM56-7B	V2531-E5	Trent 500
Thrust (lb$_f$)	27,300	31,000	54,500
Thrust-to-Weight Ratio	5.19	5.85	4.95
Length (in)	104	126	155
Diameter (in)	61	66.2	97.4
Dry Weight (lb)	5,257	5,300	11,000
Bypass Ratio	5.1	4.7	7.55

Figure 8-2 below shows a schematic of the CFM56-7B engine. The engine has a two spool compressor and is configured with 9 compressor stages. Additionally, the engine features 4 turbine stages. The combustor is laid out in an annular fashion, and the engine has been featured on many airplanes, including the C-40 and Boeing 737.
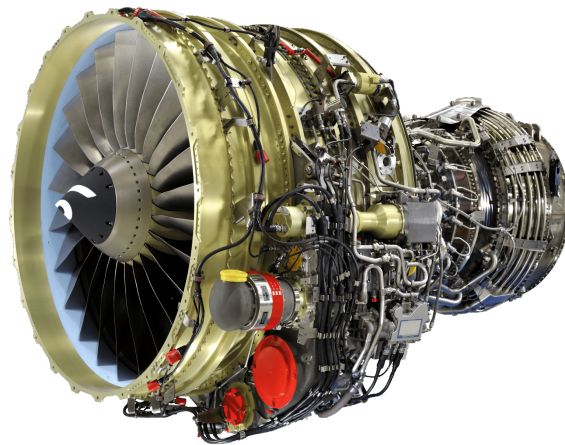
Figure 8-2. Schematic of CFM56-7B Engine

8.2 Engine Performance

      After selecting the CFM56-7B, the team developed a corresponding performance model and integrated the engine into the mission analysis. This process required four main steps: (1) gather engine data from public databases, (2) create a GasTurb model validated against that data, (3) make a conversion code to reformat the GasTurb output, and (4) analyze the mission performance with the custom engine deck in FLOPS (Figure 8-3).
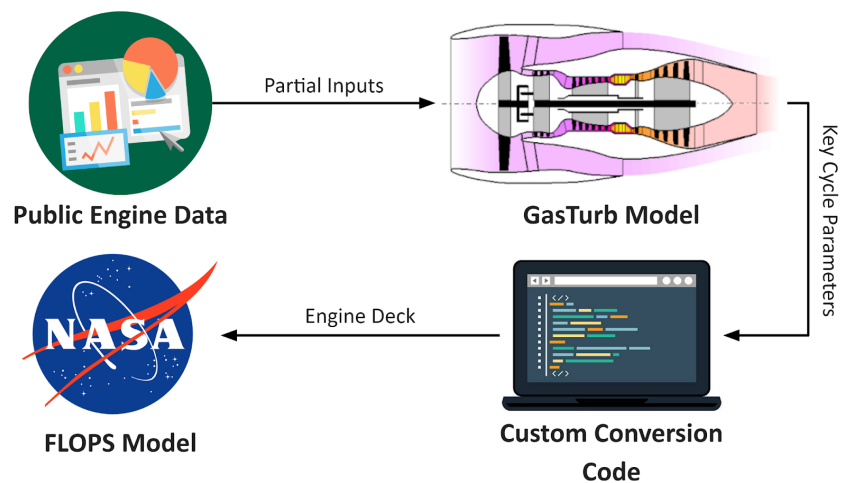
Figure 8-3. Flowchart of Engine Analysis Process

Due to the popularity of the CFM56-7B, thermodynamic cycle parameters are readily available through academic publications and government reports. Using these parameters, the team created a thermodynamic cycle model in GasTurb, a professional software for gas turbine performance calculations. The software comes with 15 predefined engine configurations: the geared turbofan was chosen to represent the CFM56-7B. After choosing the predefined configuration, the engine parameters from literature were entered into the GasTurb GUI (Figure 8-4).
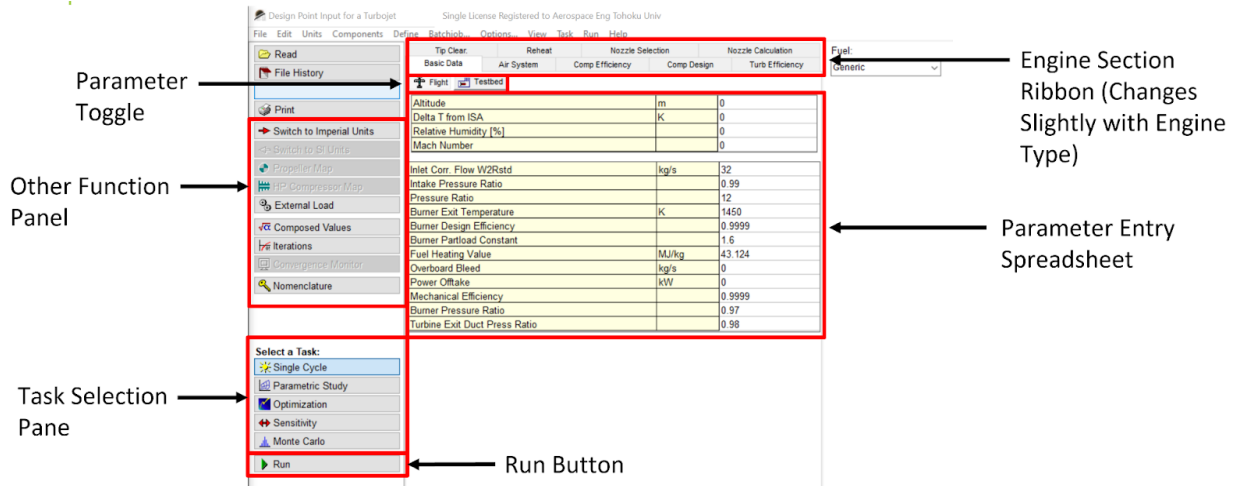
Figure 8-4. GasTurb Parameter Input Screen with Callouts

GasTurb outputs a results summary which includes mass flow rate, temperature, and pressure at different thermodynamic station numbers (Figure 8-5). The output also includes component pressure ratios, component efficiencies, and overall performance parameters.
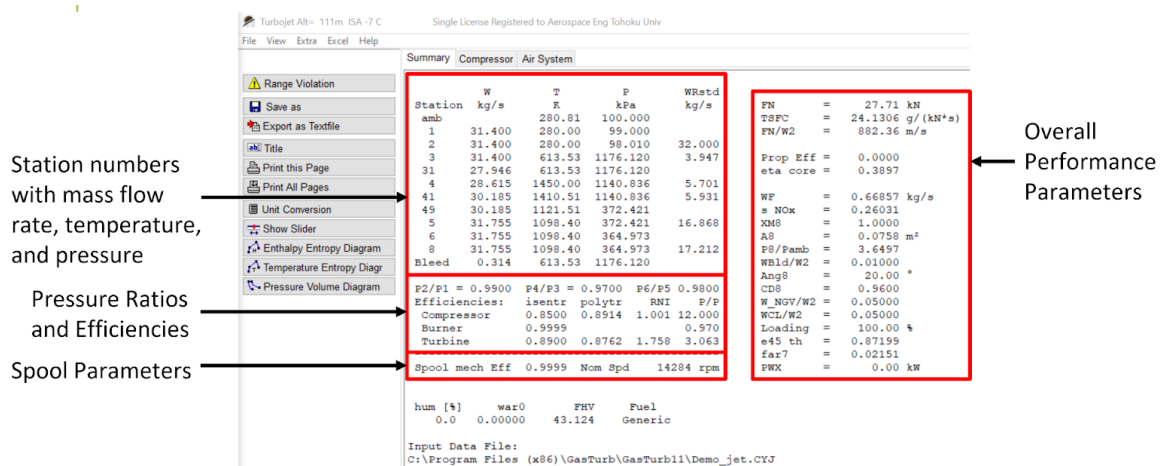
Figure 8-5. GasTurb Results Summary with Annotations

To validate the accuracy of the engine deck, the net thrust and TSFC from GasTurb were compared with available data (Table 8-2). Both parameters matched well with previously reported values. This lent considerable confidence to the GasTurb model.

Table 8-2. Comparison of TSFC and Net Thrust

	TSFC (lb/lb$_f$/h)	Net Thrust (lb$_f$)
Actual Data	0.366 – 0.376	21,580 – 24,000
GasTurb Model	0.376	23,830

Using the aforementioned custom conversion code, the GasTurb output was translated to a FLOPS engine deck. The FLOPS engine deck requires altitude, Mach number, gross thrust, fuel flow, NOx emissions index, and nozzle exit area. From the mission requirements, the team varied the altitude and Mach number from 0 to 15,000 ft and 0 to 0.7, respectively. The associated output parameters were captured using the "Parametric Study" function in GasTurb. The resulting FLOPS engine deck was used in all mission analyses presented in this report.

The engine was "rubberized" within FLOPS using two parameters, fuel flow factor and engine weight. Based on subject matter expert testimony, these parameters are sufficient to modify the engine when the net thrust and TSFC changes by less than 5%. The final values chosen for fuel flow factor and engine weight were 1 and 5,257 lb, respectively.

8.3 Airframe Integration

On top of performance analysis, engine-airframe integration is critical to airplane performance. Most commercial transport aircraft place the engines on pylons beneath and slightly forward of the leading edge of the wing. While this is a widely accepted industry standard, CFD simulations confirm that the engine locations with the least drag are above/forward and below/forward relative to the wing leading edge (Fig. 8-6). Furthermore, positioning the nacelle slightly forward of the leading edge allows the engines to ingest "clean" air, extending service life and augmenting performance.
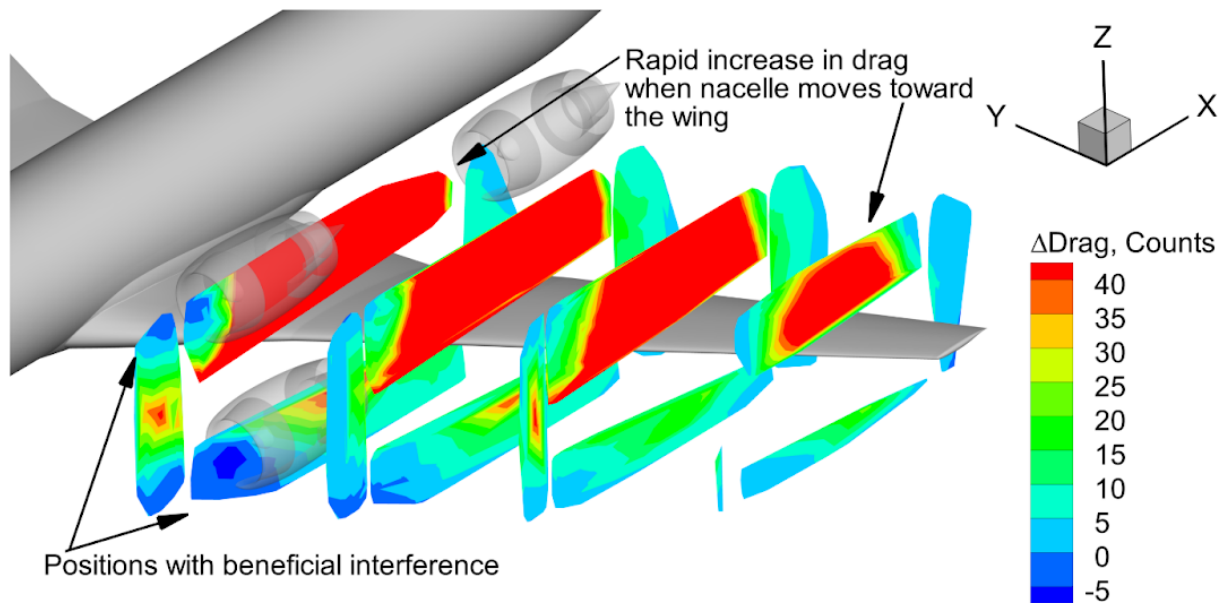
Figure 8-6. Change in Drag with Various Nacelle Placements (Blaesser, 2020)

In addition to canonical engine placements, the team considered advanced propulsion-airframe integration techniques. These methods are designed to re-energize the boundary layer on the fuselage. By creating a larger velocity gradient (and subsequent momentum gradient) across the engine, the engines can produce more thrust and decrease drag (Hall et al., 2017). However, these designs inhibit maintenance and add significant structural complexity. For those reasons, the engine was placed on pylons beneath and slightly forward relative to the leading edge of the wing. The pylons were aerodynamically contoured to reduce drag (Fig. 8-7).
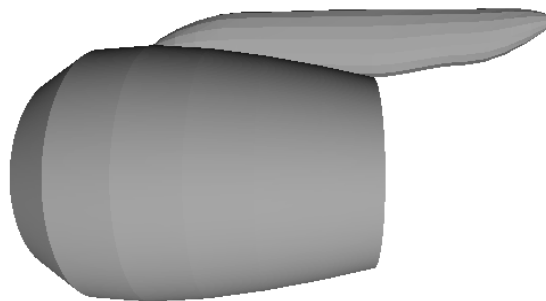
Figure 8-7. Engine Nacelle with Contoured Pylon

9. **Aerodynamics**

This section covers all of the key aerodynamic properties of the final aircraft, highlighting specifically the wing and tail design and the relevant control surfaces. The first subsection includes a description and analysis of the choices behind the airfoil selected for the wings and vertical and horizontal tails as well as the placement and style of the wing planform. After a justification of these design choices, there is an in-depth analysis of the aerodynamic performance of the entire aircraft using a combination of VSPAERO and Flightstream simulations. This section includes CAD designs for control surfaces on the wings and empennage and then discusses their effectiveness. Lastly, this section discusses high-lift technologies that are included on the aircraft, mainly the trailing-edge flaps on the wings to aid in takeoff and landing.

9.1 Airfoil Selection

Several options were considered before selecting an airfoil to carry forward for wing planform design and analysis. The team decided that a combination of a high camber airfoil for the root of the wing and a higher lifting foil at the tip would yield preferred performance. This was inspired by the wing design for the C-130H which combines the NACA 64A3418 (root) and the NACA 64A412 (tip). Naturally, these were the first airfoils considered. Additionally, the P-38's NACA 23015 (root) and NACA 4412 (tip) were chosen based on a similar cruising Mach number of approximately 0.6. The DC-10's DSMA 523B (root) was considered based on a similar payload range. Finally, the CL-415's NACA 4417 was considered along with the NACA 001 for baseline comparison. All data on lift and drag coefficients was found with Airfoil Tools at a Reynolds number of 1,000,000 and a critical number of 5 (assuming a 2D formulation). Below is a table summarizing the findings of the comparison.

Table 9-1. Comparison of C_L and C_D Metrics for Various Airfoils

Airfoil	C_l Takeoff ($\alpha = 15$)	C_d Takeoff ($\alpha = 15$)	C_l Cruise ($\alpha = 2$)	C_d Cruise ($\alpha = 2$)
NACA 001	1.42	0.31	0.23	0.009
NACA 4412	1.53	0.04	0.7	0.009
NACA 64A$_3$418	1.4	0.05	0.55	0.009
NACA 64A412	1.5	0.045	0.6	0.01
NACA 23015	1.51	0.028	0.37	0.0085
DSMA-523B	1.8	0.038	0.75	0.016
NACA 4417/8	1.51	0.045	0.67	0.01

Highlighted above are the selected airfoils. Keeping with the main inspiration of the final design, the C-130's NACA 64A$_3$418 was chosen for the root of the wing. The main difference between the final design and the preliminary design is the tip airfoil. The NACA 4412 boasts a higher max C_l and lower C_d than the NACA 64A412, making it the preferred choice.

9.2 Wing Design

The wing design has an aspect ratio of 8.94, which was determined as an optimal aspect ratio given the sizing constraints outlined in Section 7. The area of the wing was calculated to be 1,590 ft^2 in order to handle the aerodynamic loading of the weight of the aircraft, as well as store the required amount of fuel for the mission. There is a 0° sweep angle on the wings, since the aircraft will be traveling at subsonic speeds throughout the mission without the presence of shock waves. The wing is split into two sections, a smaller section with a taper ratio of 1 closer to the fuselage and the rest of the wing which has a taper ratio of 0.53. This taper ratio was chosen due to the 0° sweep angle: Raymer (1999) mentions that "most wings of low sweep have a taper ratio of about 0.4-0.5."

The wing's aspect ratio, area, sweep angle, and taper ratio were all used to determine the planform features, including the span, and the chords of the root and tip. The span of the wing is 120 ft, with a root chord of 16.2 ft and

a tip chord of 8.50 ft—giving a mean aerodynamic chord of 12.8 ft. A summary of all of the important wing

parameters are listed in Table 9-2.

Table 9-2. Summary of Wing Dimensions

Characteristic	Value
Aspect Ratio	8.94
Area (ft²)	1,590
Sweep Angle (°)	0
Taper Ratio	0.530
Span (ft)	119
Root Chord (ft)	16.2
Tip Chord (ft)	8.50
Mean Aerodynamic Chord (ft)	12.8

9.3 Aircraft Aerodynamic Characteristics

OpenVSP's complementary aerodynamic solver, VSPAERO, was used to compute the aerodynamic

performance of the aircraft. The data was validated with Flightstream, a higher fidelity solver that uses a unique

vorticity based solver. Configuration and aerodynamic analyses focused on the cruise conditions, at a Mach of 0.6.

To begin, it is first important to find the lifting coefficient of the aircraft as a function of the angle of attack, which

can be seen below in Figure 9-1.
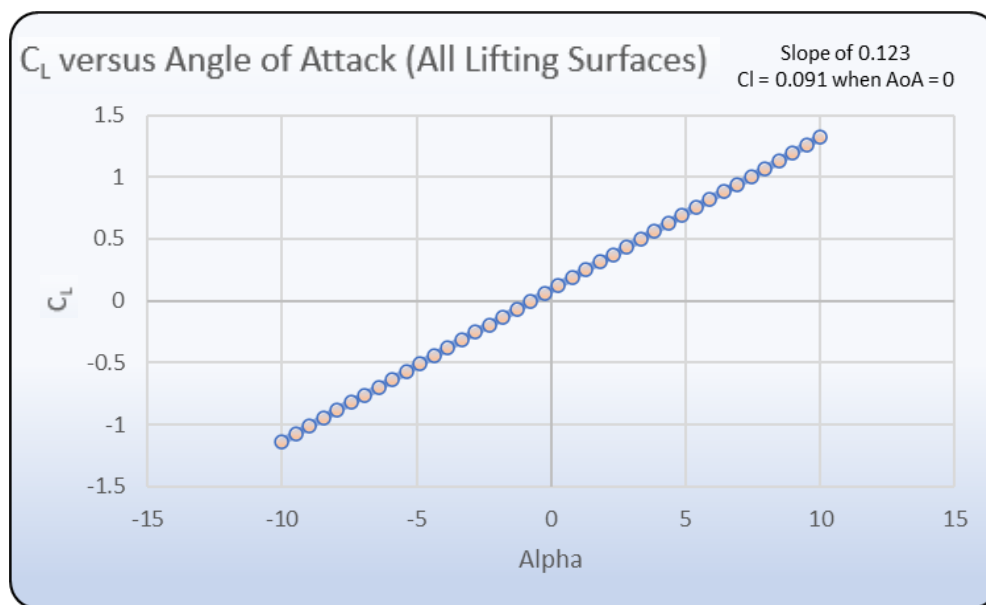
Figure 9-1. Cruise C_L versus Alpha

To determine a stall angle for the aircraft, Flightstream's vorticity-based solver was utilized and run at high angles of attack. While VSPAERO is useful for most calculations, it cannot predict stall. Furthermore, Flightstream was used to get the most accurate solution for the cruise lift coefficient, which occurs at an angle of attack of 2.0°. This trim angle was chosen for the cruise angle of attack based on historical data from similar aircraft classes. It is important to note that for the Flightstream simulations, the lifting force from the fuselage was omitted because it does not have a significant contribution relative to the wing. The results from the Flightstream simulation for stall can be seen below in Figure 9-2, accompanied by a visualization of the lifting surfaces and their trailing vortices detaching, shaded to show the free-stream coefficient of pressure at different points on the surfaces. This vortex visualization can also be seen below in Figures 9-3 and 9-4 for cruise conditions, where the cruise C_L was determined to be 1.37.
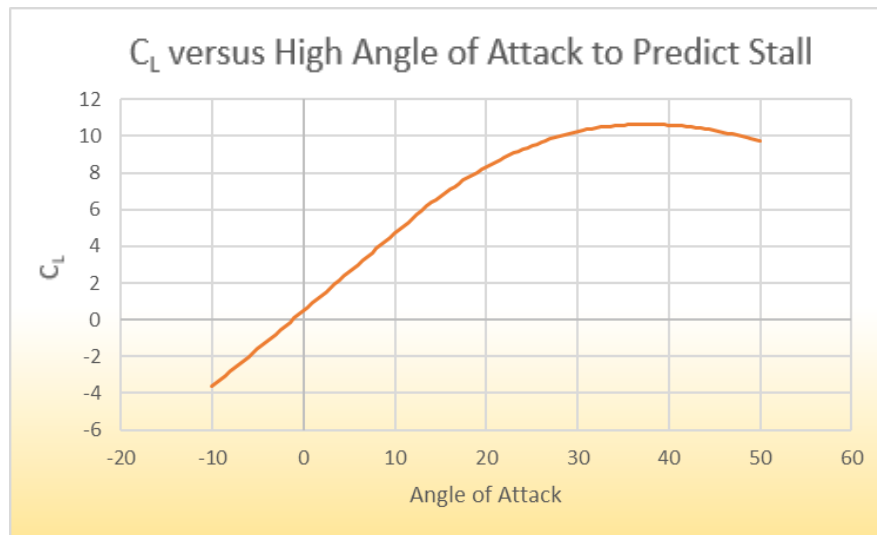
Figure 9-2. C_L versus Angle of Attack to Predict Stall
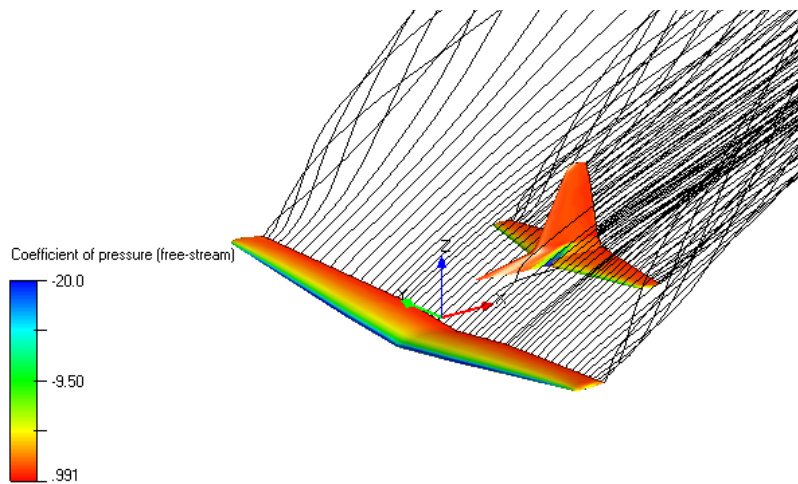
Figure 9-3. Stall Vortex Visualization
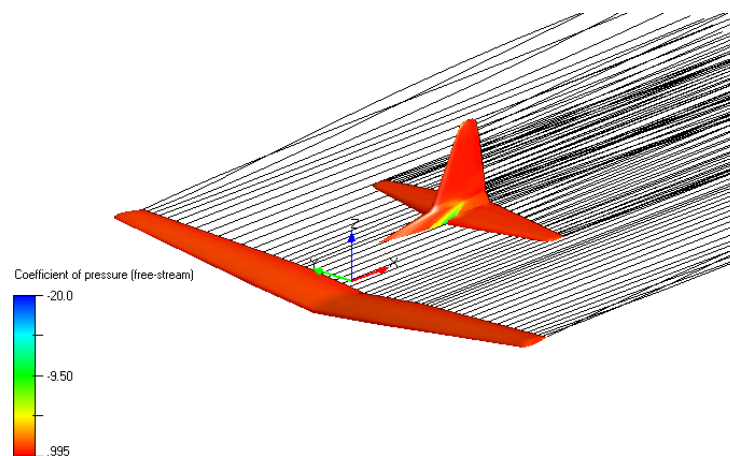
Figure 9-4. Cruise Condition Vortex and Coefficient of Pressure Visualization

Flightstream was also used to perform a number of alpha sweeps as well, attempting to find a sufficient alpha margin for operation in both the cruise and the takeoff/landing speeds to ensure the aircraft would not stall. Within a reasonable margin about the selected cruise angle and the takeoff/landing angles, stall was not predicted at any angle of attack. This ensures that the aircraft's lift capabilities will not be limited by stall at any point in the mission.

9.4 High Lift Device

In order to achieve high lift conditions for takeoff on the required field length, as well as the lift required to reach stable landing without having too high of a speed, one of the most common high-lift devices used in aircraft are flaps. The flaps chosen for the Dragonforce are slotted trailing-edge flaps, which will increase the C_L values of the aircraft while maintaining the same angle of attack by effectively increasing the camber of the wing when deflected. The devices make up the section of the wing that was not taken by the ailerons, so they extend from the fuselage to 21.19 ft outward on either side of the wing. From the guidance of Raymer (1999), the flaps have a chord that is 40% of the wing chord, 3.31 ft. On takeoff it is assumed that the flaps will deflect 25°, and on landing they will deflect 50°. The results for the flap deflection C_L curves can be seen below in Figure 9-5 and are compared against the cruise C_L for reference.
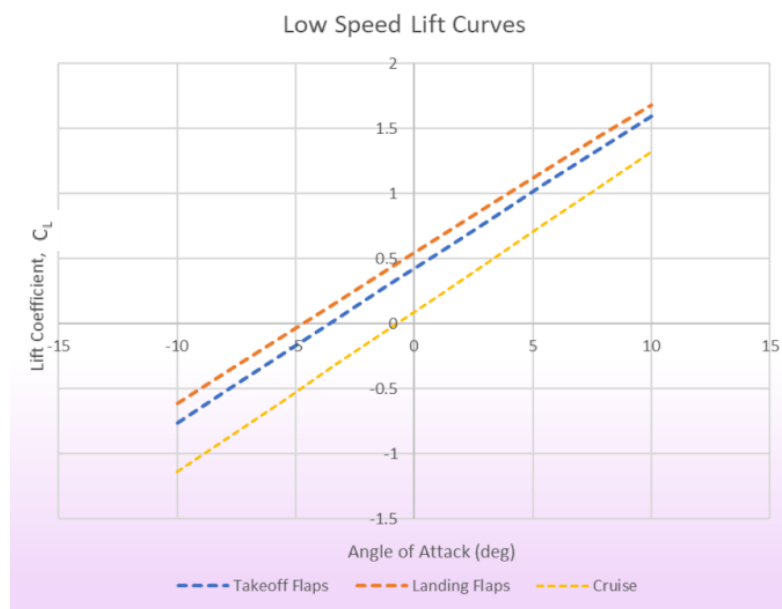
Figure 9-5. Low Speed Lift Curves for Flap Performance

Figure 9-6 below shows the layout of the control surfaces along the wing, horizontal tail, and vertical tail.
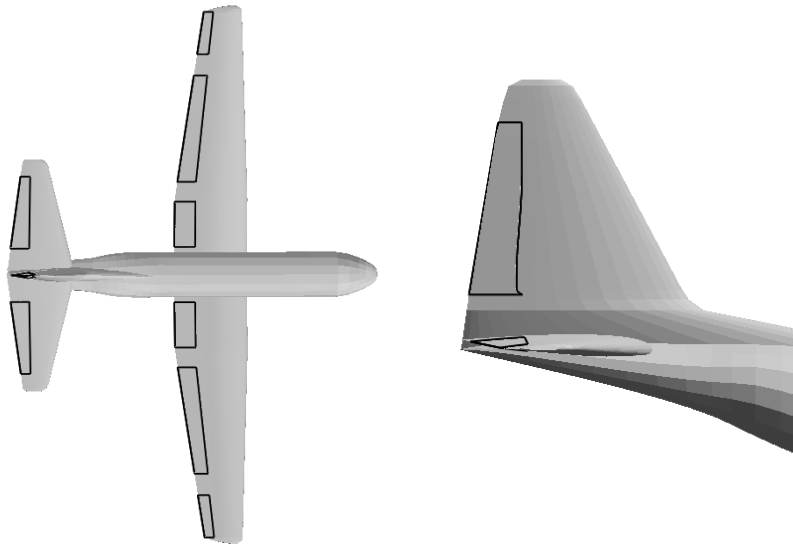
Figure 9-6. Aileron, Elevator, Flaps Overlay, and Rudder Overlay

9.6 Drag Analysis

The parasitic drag, the main contributor for drag in this subsonic aircraft, was calculated using VSPAERO's built-in parasitic drag calculator on the geometry. VSPAERO uses the Blasius Equation for the laminar C_f calculation and the Power Law Blasius Equation for the turbulent C_f calculation. The results from these calculations can be seen below in Figure 9-7. It is important to note that the wing has the largest contribution to parasitic drag, as expected, accounting for 48.9% of the total parasitic drag.

Parasitic Drag Contributions
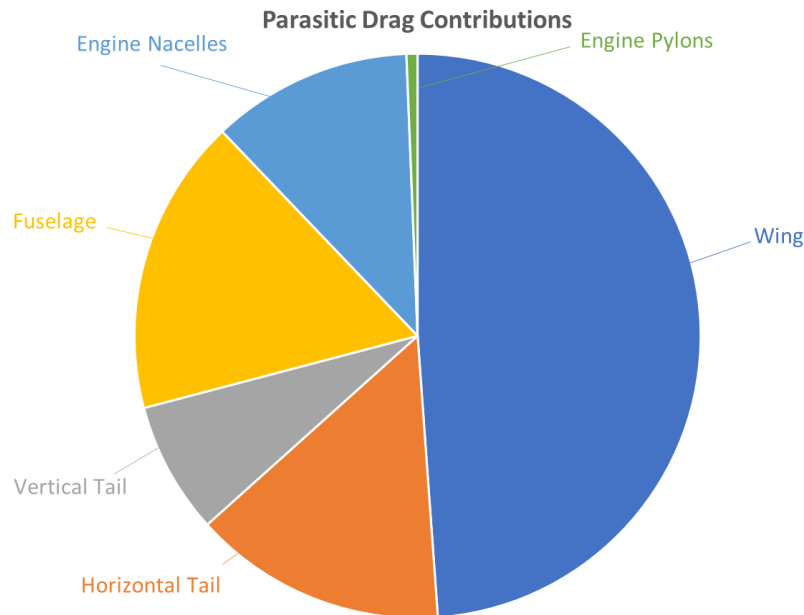
Figure 9-7. Parasitic Drag Contributions at Cruise Speed

When calculating the total drag on the aircraft, VSPAERO also calculates the induced drag, C_{Di}. The induced drag is calculated at each angle of attack primarily based on the coefficient of lift and the Oswald Efficiency Factor. The Oswald span efficiency factor, e, as discussed in Raymer (1999), is used to adjust for non-elliptical lift distributions. It is defined for unswept wings below in Equation 1.

$$e \ = \ 1.78(1 \ - \ 0.045AR^{0.68}) \ - \ 0.64 \qquad\qquad \text{Eqn. 1}$$

The e value for the Dragonforce is calculated to be 0.78, which falls within Raymer's definition of "typically between 0.7 and 0.85." This efficiency value is then used to calculate the induced drag via Equation 2 and applied to the total drag that VSPAERO calculates.

$$C_{Di} \ = \ (C_L)^2 / \pi eAR \qquad\qquad \text{Eqn. 2}$$

Figure 9-8 depicts the drag polars for various flap configurations. Furthermore, the C_L value at the minimum C_D value is marked on the plot.
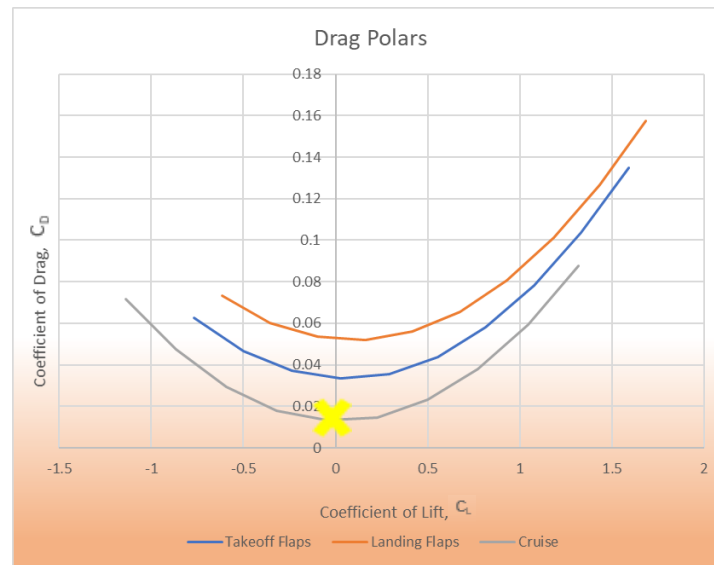
Figure 9-8: Drag Polars at Various Flap Configurations, Highlight at C_L of Lowest C_D

Finally, below in Figure 9-9 the L/D can be seen plotted against the angle of attack for various flap conditions.
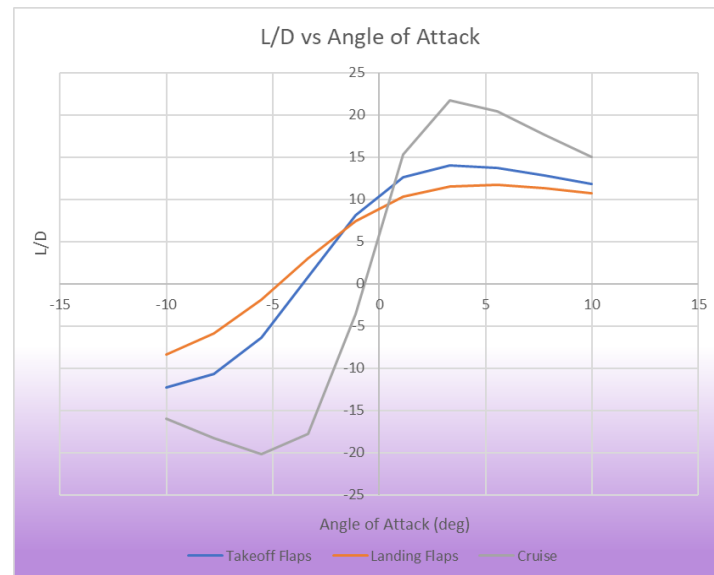
Figure 9-9: L/D plotted against Angle of Attack

10. Performance Characteristics

This section covers the flight performance characteristics of the aircraft. Analysis begins with takeoff and landing performance, where field requirements laid out in the RFP are combined with TOGW, landing weight, takeoff distance, and landing distance calculations to generate results. The results are displayed graphically, allowing the reader to visualize the team's estimation for takeoff and landing performance compared to different TOGWs and landing weights. The section details the various flight ceilings of the aircraft: absolute, service, cruise, and payload drop. These ceilings are calculated using the climb parameters detailed in the configuration and mission performance sections. Next, a flight envelope diagram is displayed, using aircraft flight weight and performance load factor to visualize the Mach number and altitude at different mission segments. In Section 10.4, the payload-range diagram is presented, providing valuable mission information.

10.1 Balanced Field Length

Balanced field length calculations were conducted at 5,000 ft mean sea level (MSL) elevation on a +35°F hot day to determine if the aircraft meets the 8,000 ft requirement. Calculations followed the procedure outlined in *The Elements of Aircraft Preliminary Design* (Schaufele, 2007) which include calculations of acceleration for three scenarios: all engines operative, one engine inoperative (OEI), and rejected takeoff (RTO). Accelerate-stop and accelerate-continue distances were calculated by plotting and integrating the $1/(2a)$ versus V^2 curves for the three scenarios (where a is aircraft acceleration and V is aircraft velocity). The balanced field length and engine failure recognition speed (V_1) were determined by finding the intersection of the plotted accelerate-stop and accelerate-continue lines (Figure 10-1).
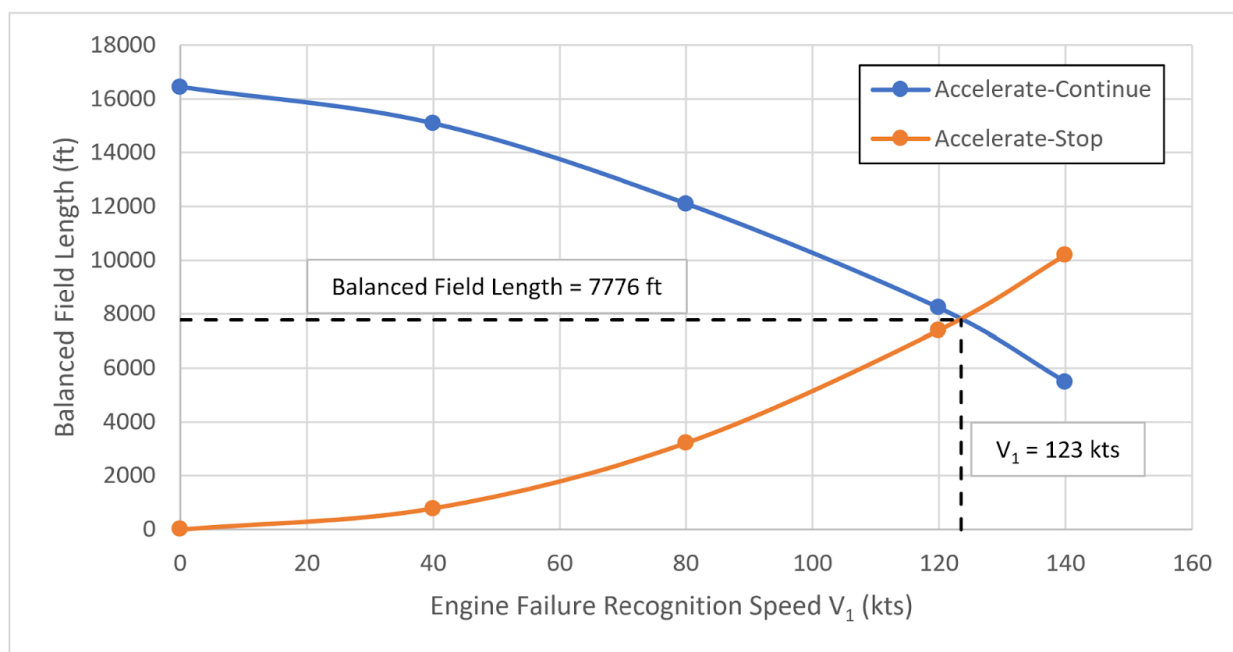
Figure 10-1. Dragonforce Balanced Field Length and Failure Recognition Speed V_1

The above balanced field length of 7,776 ft meets the 8,000 ft requirement at 5,000 ft MSL elevation on a 35+°F hot day. Because the aircraft meets the requirement offset from sea level, it also meets the requirement at standard sea level.

10.2 Design Mission Analysis

The Dragonforce is capable of performing the design mission as discussed in Section 4.3 with the payload objective of 8,000 gallons and multi-drop capability of three distinct drops of approximately 2,700 gallons each. The fuel, time, distance, Mach number, and altitudes for each segment of the mission are shown below in Table 10-1. The design mission fulfills the RFP objective of a 400 nmi design radius with full payload, with a flight time of 142.7 minutes, a block time of 2.63 hours, and a block fuel of 10,570 lbs.

Table 10-1. Design Mission Summary

Segment	Initial Weight (lbs)	Fuel (lbs)		Time (min)		Distance (nmi)		Mach Number		Altitude (ft)	
		Segment	Total	Segment	Total	Segment	Total	Segment	End	Segment	End
Taxi Out Take Off	181,797	1,650	1,650	5.0	5.0	-	-	-	0.3	-	-
Climb	180,147	1,093	2,743	4.1	9.1	21.1	12.1	0.3	0.6	0	25,078
Cruise	179,054	6,282	9,025	113.9	123.0	684.0	705.2	0.6	0.6	25,078	25,878
Release	172,771	0	9,025	0	123.0	0	705.2	0.6	0.4	25,878	13,051
Cruise	148,771	138	9,163	2.4	125.4	10.0	715.2	0.4	0.4	13,051	18,000
Release	148,634	0	9,163	0	125.4	0	715.2	0.4	0.4	18,000	18,000
Cruise	124,634	120	9,283	2.4	127.8	10.0	725.2	0.4	0.4	18,000	18,000
Release	124,513	0	9,283	0	127.8	0	725.2	0.4	0.4	18,000	18,000
Cruise	100,513	102	9,385	2.4	130.2	10.0	735.2	0.4	0.4	18,000	18,000
Descent	100,411	395	9,780	17.5	147.7	64.8	800.0	0.4	0.3	18,000	0
Approach	100,016	660	10,440	5	152.7	-	-	-	-	-	-
Taxi In	99,357	132	10,572	5	157.7	-	-	-	-	-	-

The mission analysis was computed using FLOPS, with custom segments defined to represent each part of the design mission. The three release segments represent the payload drops of approximately 2,700 gallons of retardant and are separated by cruise segments that represent either the need for the aircraft to fly to another area or loiter before the following payload drop. These cruise segments were defined for a 10 nmi distance, a Mach number range of 0.3 to 0.4, and an altitude range of 10,000 to 18,000 feet. The first cruise segment, representing the aircraft flying from base to the first drop location, was defined for a Mach number range of 0.4 to 0.6 and an altitude range of 20,000 to 28,000 feet. The segments were optimized in FLOPS to fly at the Mach number that resulted in minimum fuel flow to allow the aircraft to fly as efficiently as possible.

10.3 Ferry Mission Analysis

Additionally, the Dragonforce is capable of performing the ferry mission with no payload and fulfills the RFP objective of a 2,000 nmi design ferry range. The fuel, time, distance, Mach number, and altitudes for each segment of the mission is shown below in Table 10-2. The design ferry mission is completed with a flight time of 345 minutes, a block time of 6.00 hours, and a block fuel of 16,244 lbs.

Table 10-2. Ferry Mission Summary

Segment	Initial Weight (lbs)	Fuel (lbs)		Time (min)		Distance (nmi)		Mach Number		Altitude (ft)	
		Segment	Total	Segment	Total	Segment	Total	Segment	End	Segment	End
Taxi Out Take Off	115,103	1,650	1,650	5.0	5.0	-	-	-	0.3	-	-
Climb	113,453	711	2,361	2.8	7.8	14.2	14.2	0.3	0.6	0	28,000
Cruise	112,742	125,508	14,869	315.8	323.6	1,877.5	1,891	0.6	0.6	28,000	28,000
Descent	100,234	583	15,452	26.6	350.3	108.3	2,000	0.6	0.3	28,000	0
Approach	99,650	660	16,112	5.0	355.3	-	-	-	-	-	-
Taxi In	98,990	132	19,940	5.0	360.3	-	-	-	-	-	-

The ferry mission was computed in FLOPS after the Dragonforce was sized to the design mission of a 400 mni design radius and an 8,000 gallon payload requirement. FLOPS was rerun with the sized aircraft with zero payload and a flight range of 2,000 nmi.

10.4 Payload-Range Diagram

A payload-range diagram for the Dragonforce was developed as a result of the FLOPS mission analysis and is shown below in Figure 10-2. The three main points to note are represented by the red circles on the diagram. The first point shows that the Dragonforce is capable of carrying the full payload requirement of 72,000 lbs for a design mission radius of 800.7 nmi. At slightly over 50% of the full payload, 38,240 lbs, the Dragonforce is capable of a 4,770 nmi range which is represented by the second point on the graph. Finally, at zero payload, the Dragonforce is capable of a 5,780 nmi range.
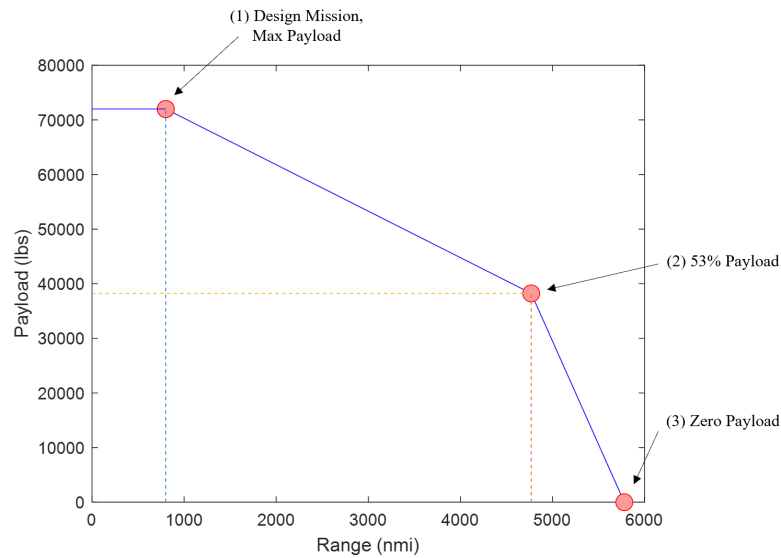
Figure 10-2. Payload Range Diagram

10.5 Flight and Service Ceilings

The flight and service ceilings were determined based on empirical data from the C-130 platform which is currently used in aerial firefighting. The absolute flight ceiling for the Dragonforce is set at 37,500 ft—directly between 33,000-42,000 ft—which are the absolute flight ceilings for C-130 (33,000 ft) and commercial aircraft (42,000 ft) (Romano, 2022). The cruise ceiling is set at 28,000 ft in order to optimize fuel efficiency given the TOGW and payload size of the Dragonforce. When in the firefighting phase of the mission profile, the flight ceiling is 1,500 ft during cruise, which is the normal altitude zone for large air tankers when firefighting. Additionally, the flight ceiling is 400 ft when dropping retardant in order to follow the RFP objectives. The Dragonforce was designed and tested to perform at the following flight ceilings tabulated in Table 10-3 below.

Table 10-3. Flight Ceilings

Ceiling Type	Altitude (ft)
Absolute	37,500
Service	28,000
Firefighting	1,500
Retardant Drop	400

11. Stability and Control

This section covers the empennage design and sizing, control surface sizing, analyses of static stability, and a sensitivity analysis of these analyses. The Empennage Design Section includes a trade study to detail which configuration was chosen for the final design. This trade study applies a Quality Function Deployment (QFD) ranking scale to various categories such as cost, size, stability, and weight. The Empennage Sizing Section includes the methodology for empennage sizing and key characteristics of both the vertical and horizontal stabilizer. The Control Surface Sizing Section includes characteristics of the aileron, rudder, and elevator and justification for these values . The section covering static stability contains methodology, figures demonstrating conventions used for positive angles and axes for analyses, key values (e.g. neutral point location, CG location, static margin, aerodynamic center, etc.), and descriptions of stability performance.

11.1 Empennage Design

A trade study was conducted in order to determine the final empennage design. As shown in Table 11-1, the team applied a system of weights based on the importance of each parameter with regards to the mission and the RFP. These weights were then applied to each of the five tail configurations based on the performance abilities of each found in Roskam (1985). The tail configurations that were compared were a conventional tail, t-tail, cruciform tail, h-tail, and pi-tail. The parameters that the different tails were judged by were, from highest to lowest, cost, weight, stability, and size.

Table 11-1. Weighted Study of Various Tail Configurations

Category	Weight	Conventional Tail	T-Tail	Cruciform Tail	H-Tail	Pi-Tail
Stability	2	2	3	1	5	4
Weight	3	5	2	4	1	3
Cost	4	5	4	3	2	1
Size	1	5	1	4	2	3
Total	-	44	41	27	23	31

After ranking each tail configuration and adding up the weighted scores, the conventional tail configuration surpassed all others, so it was implemented in the final design.

11.2 Empennage Sizing

The tail sizing process heavily relied on the tail volume coefficients as well as the length between the center of gravity and the quarter chord for both the horizontal and vertical tail. Since the Dragonforce is modeled off of the C-130, the tail volume coefficients for the C-130 were calculated based on the geometry of the aircraft. From that, the comparative sizes of the Dragonforce's horizontal and vertical tail were calculated with the adjusted sizes of the wing and fuselage length, making them different from that of the C-130. The final design utilizes the C-130 vertical tail airfoil of a NACA 64a016 and has a NACA 23012 as the horizontal tail airfoil.

11.3 Control Surface Sizing

The control surfaces were sized based on the guidance from historical data provided by Raymer (1999). The ailerons are both 44.5 ft long and have a chord length of 4.6 ft. This makes them have a Total Aileron Span to Wing Span ratio of 0.37, and a Aileron Chord to Wing Chord ratio of 0.3. This is in accordance with Figure 11-1, by Raymer. The ailerons extend to about 93% of the wingspan, ending 8.20 ft from the wing tip. Note that the ailerons do not extend to the wingtip because they would provide little control advantages at this length due to wingtip vortex effects, so the additional 7% of wing at the end of the aileron does not need to be used. The flaps make up the rest of the wingspan on either side of the fuselage, spanning 12.43 ft with a chord length of 6.46 ft, or 40% of the wing chord to provide for the largest lift contributions when deployed. The rudder extends to 90% of the vertical tail wingtip and begins right at the end of the fuselage, for a length of 18.48 ft. Its chord is 25% of the tail chord, at 4.07 ft. The elevators also extend to about 90% of the horizontal tail, extending 22.70 ft and ending 2.59 ft from the tip with a chord of 32% of the horizontal tail chord, or 4.56 ft.
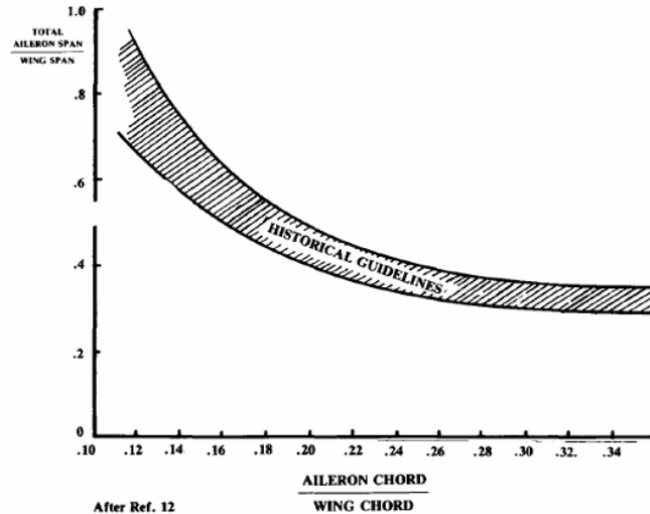
Figure 11-1. Historical Aileron Sizing Guidelines (Raymer, 1999)

11.4 Static Stability

Longitudinal static stability analysis was conducted using VSPAERO. The analyses were performed using cruise conditions of Mach 0.6. The horizontal stabilizer incidence angle (i_H) was selected to be -3.8° in order to obtain an aircraft trim angle of approximately 2°. Trim angle was determined to be 2.05° by graphing C_m versus angle of attack (AOA) (Figure 11-2). Due to favorable values of the longitudinal stability derivative C_{m_α} (-2.39) and static margin (0.27, see Section 13.2), the Dragonforce is highly longitudinally stable.
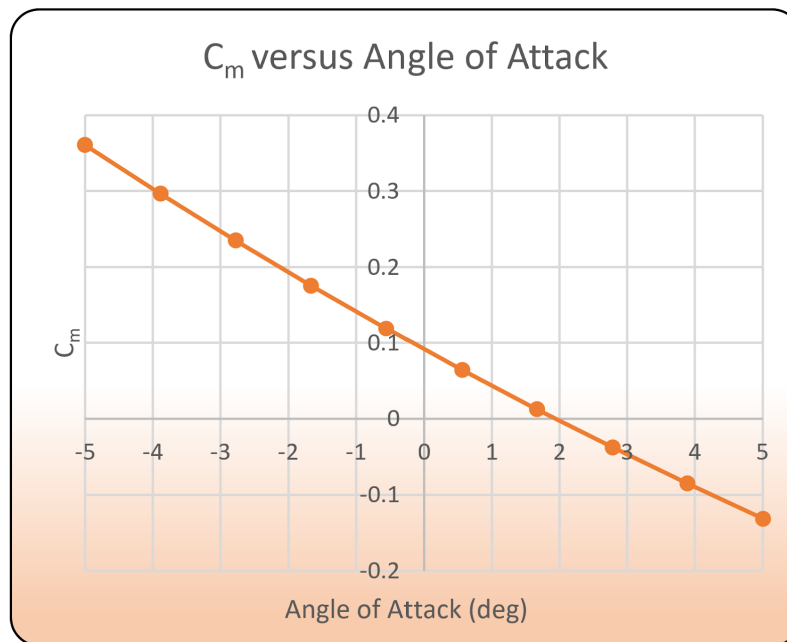
Figure 11-2. Aircraft Longitudinal Stability and Trim Angle

Lateral and directional static stability analyses were conducted through VSPAERO at cruise conditions of Mach 0.6. The favorable values of the lateral and directional stability derivatives (C_{l_β} = -0.1 and C_{n_β} = 0.1, respectively) indicate that the aircraft is both laterally and directionally stable.

12. Structures and Loads

This section of the report highlights the loads experienced by the aircraft, material selection, landing gear design to support such loads, and the service life of the aircraft. The loads subsection focuses on the maximum wing loading calculation and presents a wing skeletal CAD model. The model shows maximum deflection and shear stresses under maximum wing loading. This section also includes a V-n diagram to represent the maximum loads considered for airframe sizing and design. Using the calculated loads, appropriate materials are chosen for the fuselage, wing, and landing gear. This section includes information on the materials—such as a summary of material properties and evidence that these materials will sustain the various flight loads. Additionally, the landing gear design is discussed in this section, including the specifications of the final design. Finally, the section touches on the service life of the Dragonforce because it is partially a function of the loads that the aircraft has experienced.

12.1 V-n Diagram

The aircraft V-n diagram was generated following the guidelines set in Federal Aviation Regulation (FAR) Part 25 to determine key design speeds and load factors to be used in wing loading and structural analysis (see Section 12.2). Design speeds plotted include maneuvering speed (V_A), maximum gust intensity speed (V_B), cruising speed (V_C), dive speed (V_D), 1-g stalling speed (V_{S1}), and negative load factor stall speed (V_{Sneg}). Gust lines were generated with V_C gusts of 56 ft/s and V_D gusts of 28 ft/s. Figure 12-1 displays the complete V-n diagram.
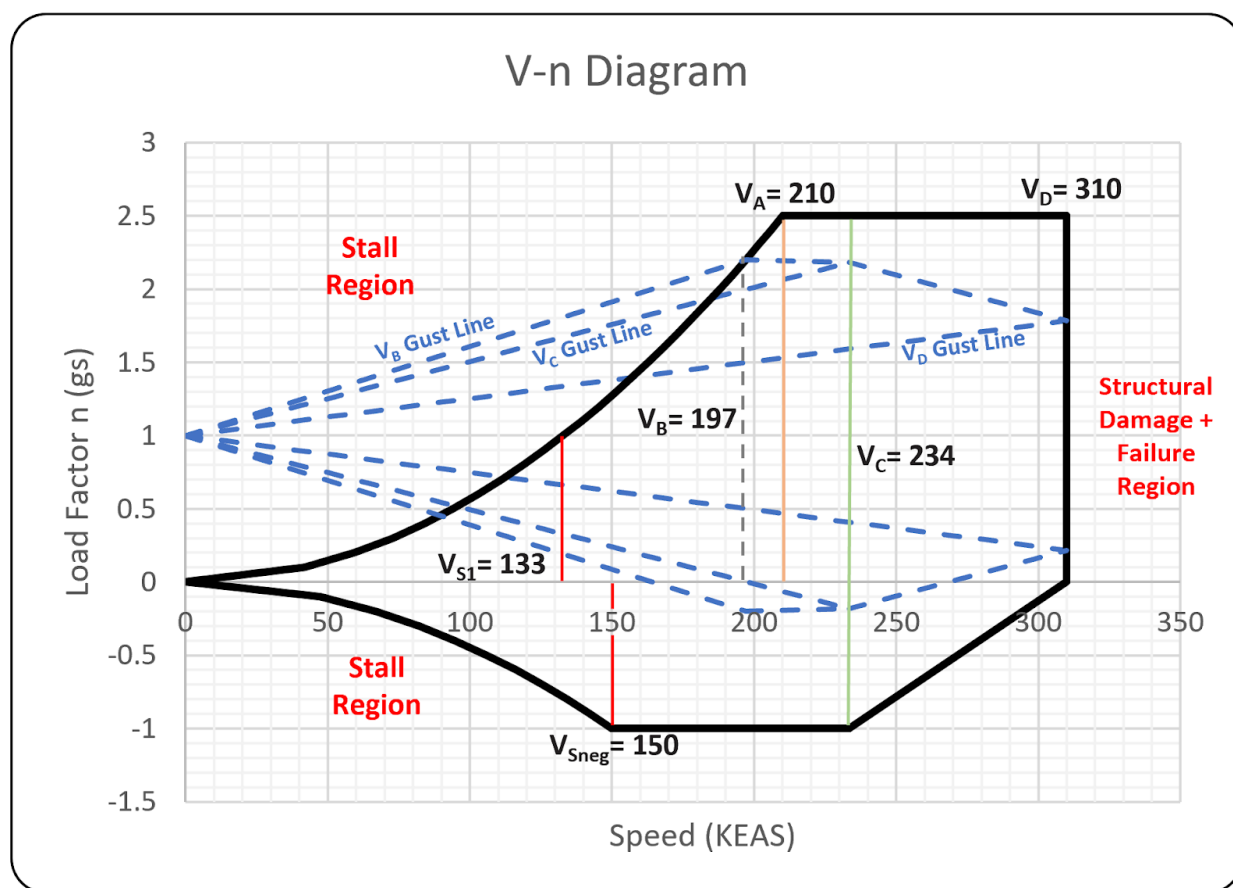
Figure 12-1. Dragonforce V-n Diagram with V_C Gust Speed = 56 ft/s and V_D Gust Speed = 28 ft/s

12.2 Wing Loading and Structural Analysis

12.2.1 Wing Loading Cases

In order to verify wing structural integrity, wing loading was analyzed during cruise, a 2.5g pull-up maneuver, and a 1g dive maneuver. These "g"s are the load factor the aircraft experiences, based on multiples of acceleration due to gravity. Cruise has a load factor of 1, the pull up maneuver has a load factor of 2.5, and the dive maneuver has a load factor of -1. The TOGW was used as the total applied load, and a factor of safety of 1.5 was applied for all cases. Since the load will be identical on each side of the aircraft, the lift and weights are only calculated for one wing. These load cases were calculated using Schenek's Approximation, which assumes the spanwise lift distribution is equivalent to the average between an elliptical and trapezoidal lift distribution, both of which are found below. For both equations, *n* is the load factor, *y* is the distance from the root chord, *L* is total lift applied to the wing, and *b* is the wing span. For the trapezoidal wing, λ is the wing taper ratio.

$$L_{ellip}(y) = n\frac{4L}{\pi b}\sqrt{1 - [\frac{2y}{b}]^2} \qquad\qquad \text{Eqn. 3}$$

$$L_{trap}(y) = n\frac{2L}{b(1+\lambda)}[1 - \frac{2y}{b}(1 - \lambda)] \qquad\qquad \text{Eqn. 4}$$

To calculate the lift on the wing, the elliptical and trapezoidal lifts were averaged and plotted against other external loads on the wing. Since the only difference between the load cases is the load factor, only the lift curve for the cruise load case is depicted in Figure 12-2. During flight, there are a few other significant loads. The structural weight of the wing was plotted based on total weight of the wing structure from FLOPS and the planform area. The fuel weight of the wing was based on a total capacity of 1,212 gallons distributed along the four baffles where the fuel tanks are located. Finally, the engine weight is located 16.67 ft from the root chord, which is where the wing begins to taper. These are all depicted in Figure 12-3. The total load was found by subtracting the structural wing loading curve from the lift wing loading curve and plotting the result. These are shown for all three load cases in Figure 12-4.
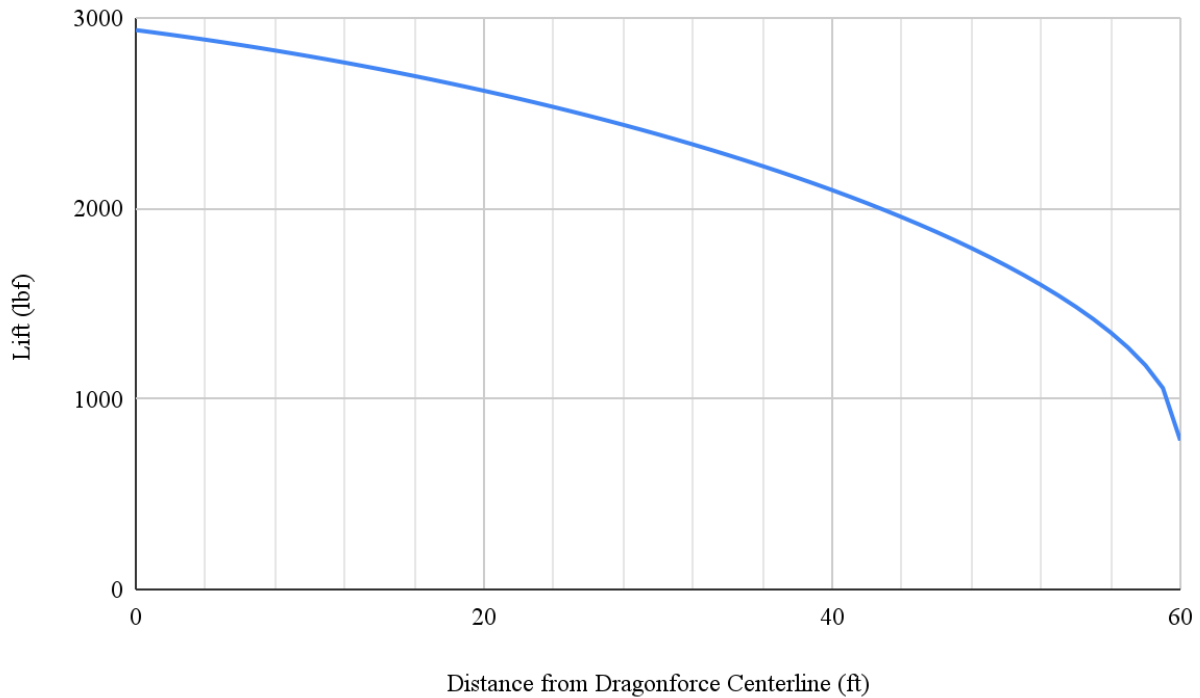
Figure 12-2. Distributed Lift on Wing for Cruise Load Case
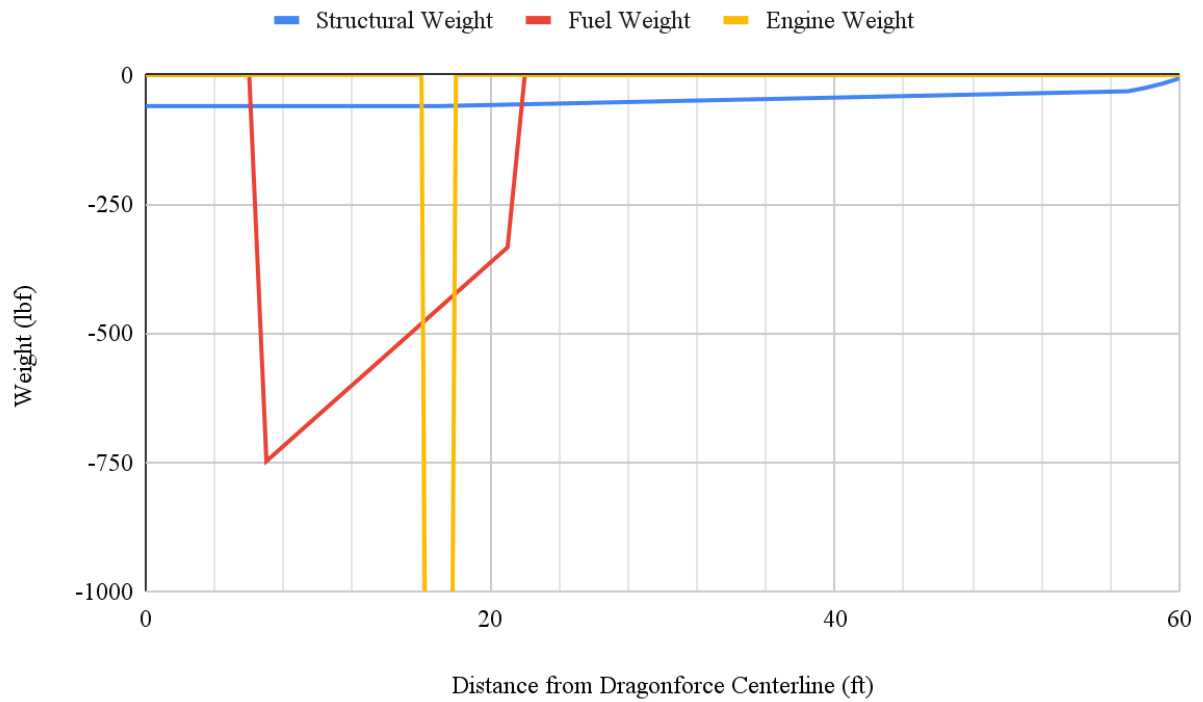
Figure 12-3. Structural and Fuel Loads
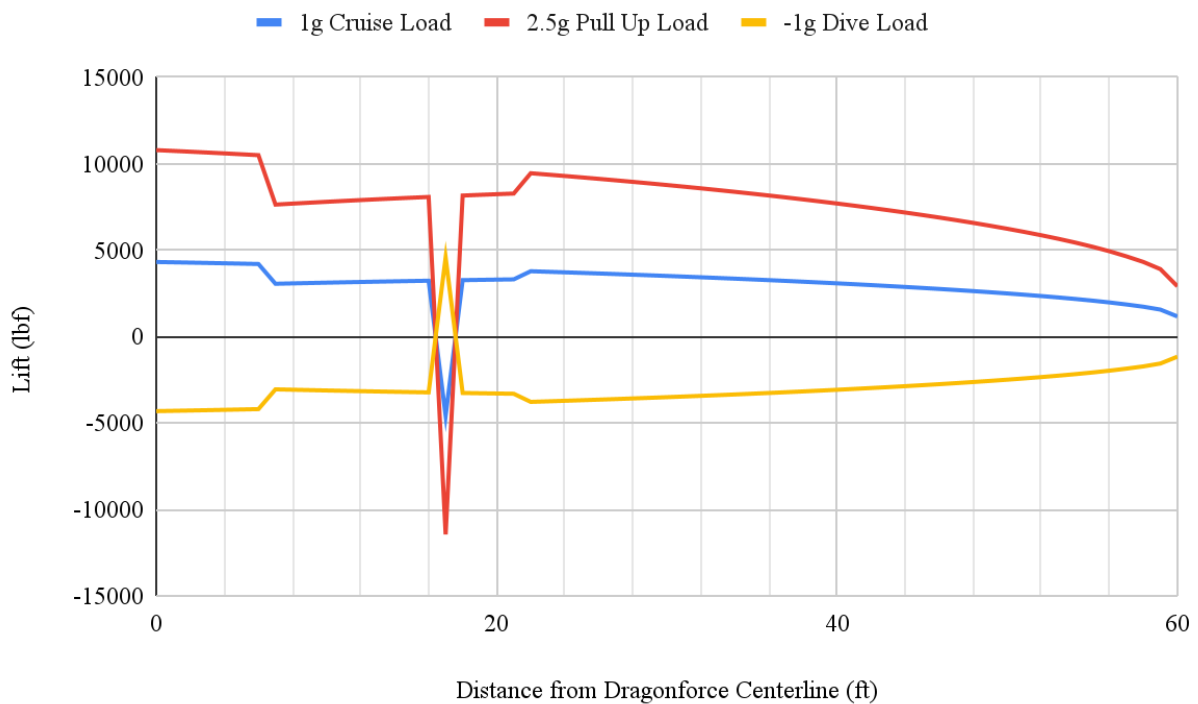
Figure 12-4. Distributed Load for All Load Cases

Integrating the total load on the wing results in the three shear diagrams plotted in Figure 12-5. The maximum shears were 180 kip, 450 kip, and -180 kip for cruise, +2.5g maneuver, and -1g maneuver, respectively. Integrating the shear diagrams gives the moment diagrams for the load cases shown in Figure 12-6. The maximum moments were 4,942 ft-kips, 12,356 ft-kips, and -4,942 kips for cruise, +2.5g maneuver, and -1g maneuver respectively, all at the root of the wing.
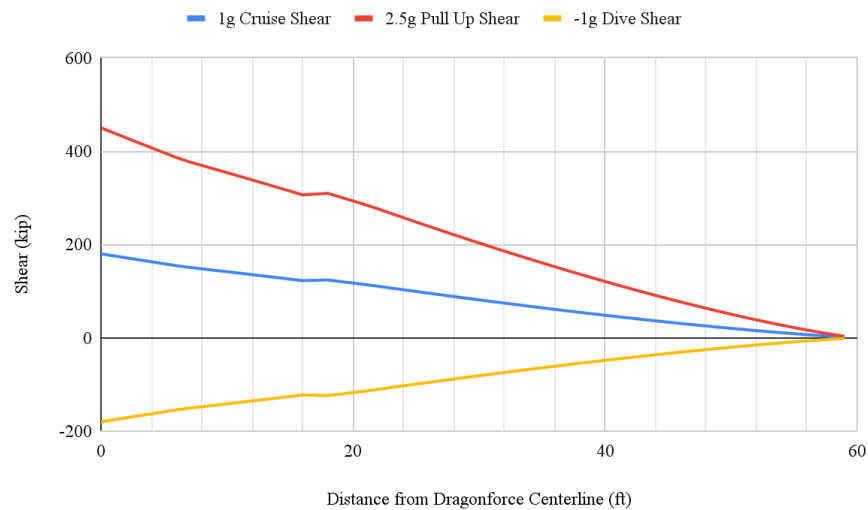
Figure 12-5. Shear Diagrams for All Load Cases
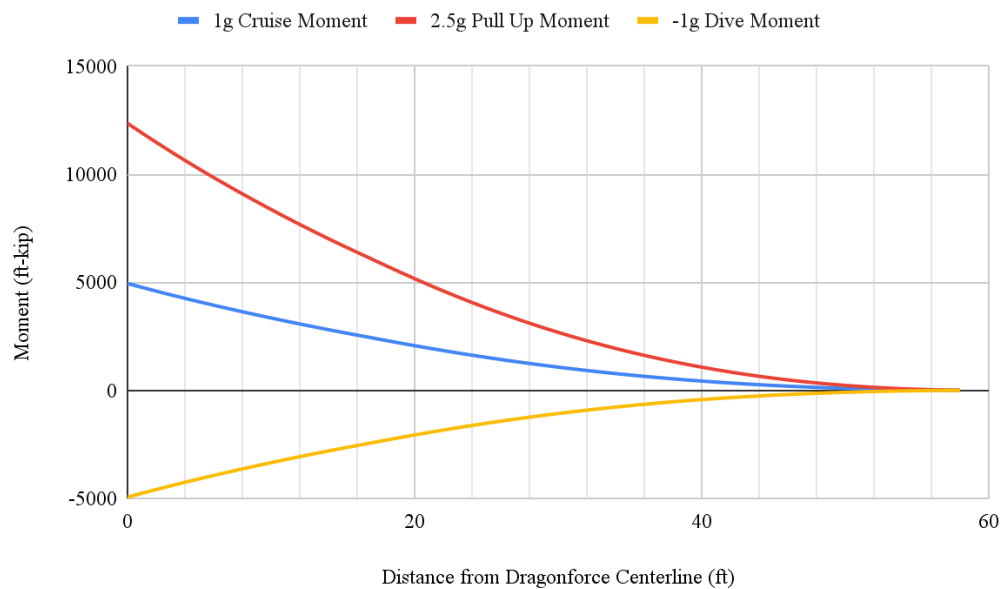
Figure 12-6. Moment Diagrams for All Load Cases

12.2.2 Internal Wing Structure

The internal wing structure can be found in Figure 12-7. The individual spars are ¾ in thick and spaced 3.5 ft apart. The front and rear spars are each 2 ft thick. The front spar spans from the root quarter chord to the tip quarter chord, while the rear spar spans from $0.65c_{root}$ to $0.7c_{tip}$ to accommodate the ailerons and high lift devices.
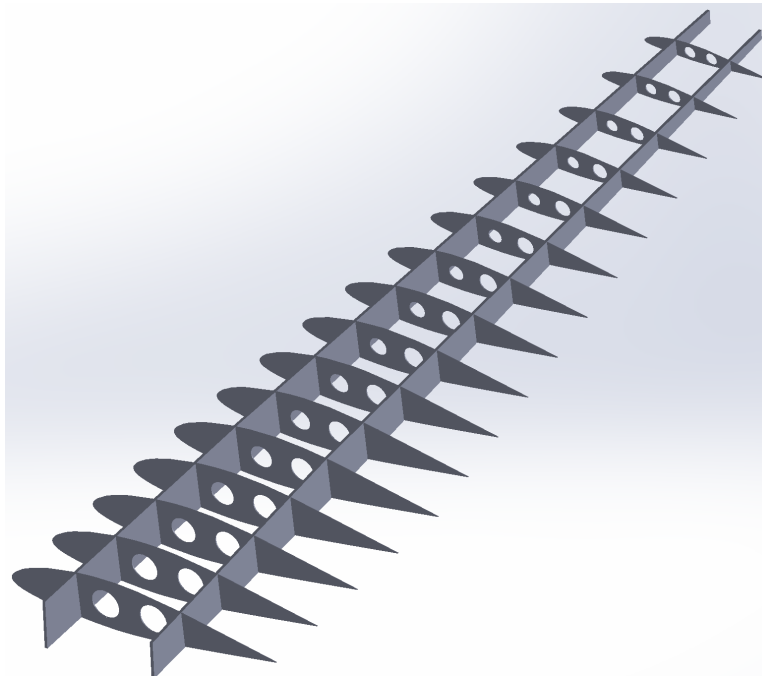
Figure 12-7. Internal Wing Structure

12.3 Material Selection

The materials for the aircraft fuselage were primarily selected based on estimated loading and comparison to existing aircraft. The fuselage frame will use Aluminum 7075-T6, which is commonly used in aerospace applications for its low density and corrosion resistance (Asmatulu, 2012). The external skin will use a carbon-fiber-reinforced polymer (CFRP), which are widely used in the aerospace industry for their strength, stiffness, and light weight. The fuselage skin will use a carbon laminate composite similar to those present on the Boeing 787, with epoxy serving as the binding polymer. CFRPs also have excellent corrosion resistance, which will be beneficial on the bottom of the fuselage since fire retardant corrodes aluminum (FAA, 1995). The high moments generated by the wings will require a strong fuselage-wing carry-through structure, so Titanium 6A1-4V will be

strategically used in this section for its superior strength and ductility. This material will also be used in the cockpit window frame to account for stress concentrations present in the windows (Inagak et al., 2014).

The materials for the aircraft wings were also selected based on estimated loading and comparison to existing aircraft. The wing spars and ribs will be made from Aluminum 7075-T6, while the wing skin will be made from the same CFRP used on the fuselage skin. This composite material will allow for greater flexibility in the wing, while the aluminum will ensure the wing remains structurally stable. These materials will also be used in the empennage.

For cost and ease of maintenance, the Dragonforce's landing gear is based on the main and nose landing gears for the Airbus single-aisle aircraft family landing gear. These landing gear from Safran Landing Systems are currently used on aircraft with maximum takeoff weights ranging from 150,000 lbs to 213,800 lbs (Modern Airliners, 2022). The structural members have high strength demands, especially during maximum takeoff weights and high impact loads during landing. Therefore, the material used must have high yield strength, fatigue strength, and good fracture toughness (Behera & Mallick, 2020). The actual materials used in Safran's landing gear are unavailable to the public, but Jeevanantham et al. (2017) found in their landing gear loading analysis that Titanium 10-2-3 (Ti-10V-2Fe-3Al) performed better than other steel and titanium alloys tested. Therefore, it is assumed and recommended that Ti 10-2-3 is used for the Dragonforce's landing gear (Inagak et al., 2014).

Ultimately, the Dragonforce uses a mix of materials that provide specific benefits to their associated components. The chosen materials and their properties are summarized in the table below.

Table 12-1. Summary of Key Materials, Uses, and Properties

Material	Used In:	Density (lb/ft³)	Tensile Strength (psi)	Yield Strength (psi)	Young's Modulus (psi ×10⁷)
Al 7075-T6	Fuselage Frame, Wing Spars, Wing Ribs	190	81,221	69,618	1.015
CFRP	Fuselage Skin, Wing Skin	125	87,022	—	0.189
Ti 6Al-4V	Carry-Through Structure, Cockpit	276	138,000	128,000	1.65
Ti 10V-2Fe-3Al	Landing Gear	290	141,000	131,000	1.60
S-Glass	Nose Cone	155	688,929	—	1.29

12.4 Landing Gear

The tricycle-style landing gear was chosen for the Dragonforce. Tricycle landing gear provides a stable configuration and is commonly used on transport aircraft. The landing gear is retractable to improve flight efficiency. The team considered two types of retraction, (1) hydraulic actuators and (2) fuselage doors (Figure 12-8). Hydraulic actuators allow for longer landing gear and can be placed within the wing if needed. On the other hand, fuselage doors do not require long poles connecting the wheels to the fuselage. Due to the high-bypass turbofan engines used on the Dragonforce, the team decided to use hydraulically actuated landing gear.

Figure 12-8. Landing Gear Retraction Mechanisms: Hydraulic Actuators (Left) and Fuselage Doors (Right)

After selecting hydraulically actuated landing gear, several key dimensions were required: distance from nose, distance from centerline, and length (Table 12-1). The main gear distance from the nose was chosen based on the CG location. When landing, the main gear needs to be aft of the CG to ensure the resultant moment brings the nose of the plane towards the ground. This requirement is satisfied since the main gear is 39.9 ft from the nose and the CG is 33.13 ft from the nose. Furthermore, the main gear was placed beneath the wing for configuration purposes. Similarly, the nose gear distance from the nose was chosen as far forward as possible to ensure maximum stability in the tricycle configuration. Likewise, the main gear was placed 6.1 ft from the centerline of the Dragonforce to prevent tipping in the lateral direction.

Table 12-2. Key Landing Gear Dimensions for Nose and Main Gear

Characteristic	Nose Gear	Main Gear
Length (in)	65	65
Distance from Nose (ft)	10.3	39.9
Distance from Centerline (ft)	0	6.1

To account for CG movement and provide margin for error, the length of the landing gear was sized such that the maximum takeoff angle was 23°, which is sufficient to prevent tail strikes on takeoff and landing. Figure 12-9 below shows a graphical depiction of the maximum takeoff angle.

Figure 12-9. Dragonforce Maximum Takeoff Angle

CAD renderings of the landing gear are shown in Figure 12-10. Both sets of landing gear vertically retract and fold into the fuselage. The Dragonforce is equipped with two hydraulic systems to facilitate landing gear movement. Additionally, the relatively simple design of the landing gear reduces repair costs and augments system robustness.
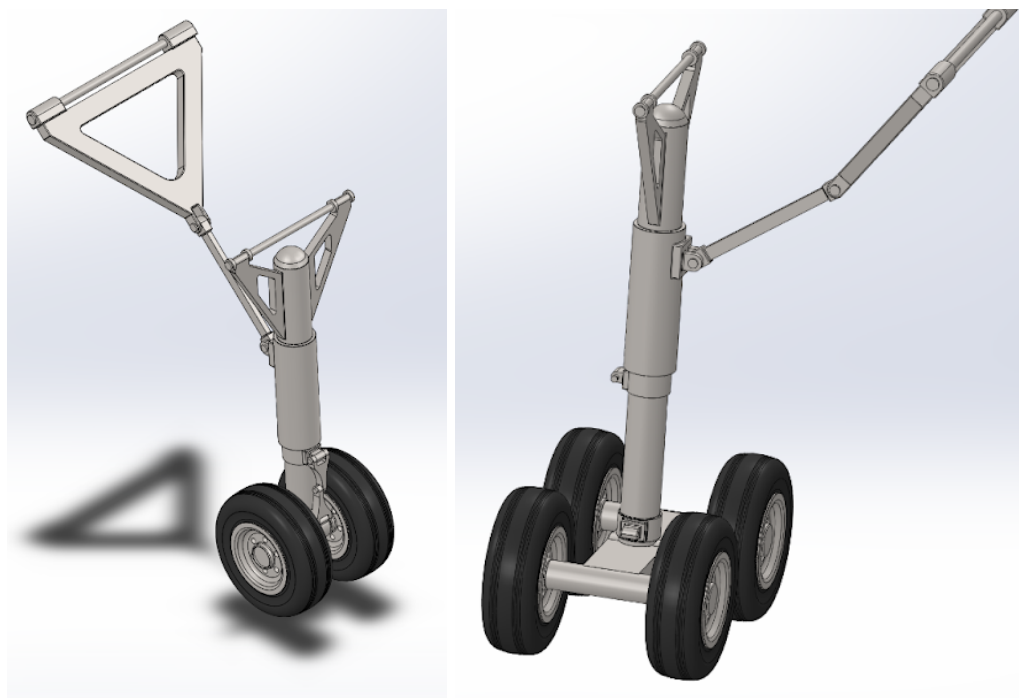
Figure 12-10. CAD Renderings of Landing Gear: Nose Gear (Left) and Main Gear (Right)

Tires are another integral part of the landing gear. Based on tire charts and aircraft requirements, the Goodyear 467Q02-3 tire was selected, with a width of 17.7 in, a diameter of 47.5 in, and a rated load of 46,000 lb_f (Goodyear, 2018). By summing the moments about the CG, the static load on each of the main gear tires was determined to be 12,800 lb_f. The extra margin between the rated and calculated loads is intended to compensate for the additional forces experienced in taxi, take off, and landing.

12.5 Service Life

According to the RFP, the Dragonforce will be used for approximately 1,200 flight hours per year for an assumed service life of 15 years. These flight hours include training, ferry, and operational flights, which are speculated to be 40% training, 10% ferry mission, and 50% design mission flights. This corresponds to 480 training hours, 120 ferry mission hours, and 600 design mission hours each year. The exact number of flights before structural failure can be estimated using Goodman's criterion, but certain characteristics of the Dragonforce were chosen with this flight hour requirement in mind. Design aspects such as the traditional empennage, simple tanks,

off-the-shelf parts, and easily available materials were chosen to provide simplified maintenance and construction,

along with increased longevity of the aircraft and its parts.

13. Mass Properties

The Mass Properties Section includes information about aircraft weight and CG locations. The first section, weight breakdown, provides a final table showing the weight of each component and total values. The Center of Gravity Section reports the values of aircraft CG and neutral point. Additionally, CG travel throughout the mission is discussed, culminating in a visual depiction of the CG travel with respect to the wing MAC.

13.1 Weight Breakdown

A weight breakdown of the Dragonforce can be seen below in Table 13-1. The breakdown is estimated using FLOPS software, and includes the total weight and breakdown of three main categories: structures, systems and equipment, and propulsion. The table also includes values for empty weight, operating weight, zero fuel weight, and the gross weight.

Table 13-1. Aircraft Component Weight Breakdown

Component	Weight (lbs)	Percentage	Component	Weight (lbs)	Percentage
Wing	19,524	10.74	Engines	11,718	6.45
Horizontal Tail	2,784	1.53	Miscellaneous Systems	386	0.21
Vertical Tail	1,722	0.95	Fuel System	705	0.39
Fuselage	10,877	5.98	**Propulsion Total**	12,810	7.05
Nacelle	985	0.54	**Weight Empty**	78,657	43.26
Structure Total	44,960	24.73	Crew	1,125	0.62
Surface Controls	1,945	1.07	Unusable Fuel	352	0.19
Auxiliary Power	406	0.22	Engine Oil	133	0.07
Instruments	482	0.27	Cargo Containers	13,330	7.32
Hydraulics	691	0.38	**Operating Weight**	93,567	51.47
Electrical	1,467	0.81	Retardant Payload	72,000	39.60
Avionics	1,715	0.94	**Zero Fuel Weight**	165,567	91.07
Furnishings and Equipment	3,270	1.8	Mission Fuel	16,238	8.93
Air Conditioning	728	0.4	**Gross Weight**	181,805	100.0
Anti-Icing	183	0.1			
Systems and Equipment Total	10,887	5.99			

13.2 Center of Gravity

Aircraft component weights were gathered from the FLOPS model (see Section 6.4). Aircraft CG, calculated from balancing the moments generated from the aircraft components, is 33.13 ft aft of the nose at TOGW. The neutral point, found from VSPAERO stability analysis, is located 36 feet aft of the nose. This combination of CG and neutral point gives a static margin of 0.27.
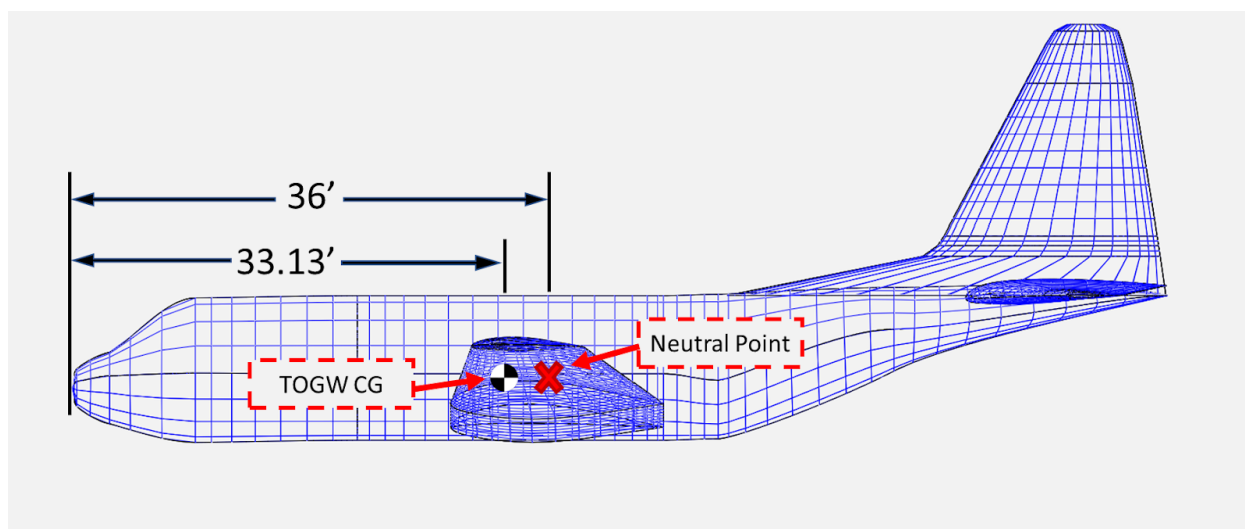
Figure 13-1. Aircraft CG and Neutral Point

13.3 CG Travel with Fire Retardant Drops and Flight CG Envelope

The fire retardant tanks were centered about the CG to minimize CG travel with fire retardant drops. This feature, combined with fuel placed in the wings, minimizes CG travel throughout the entire mission. The flight CG envelope below was developed by determining the CG with various combinations of fuel and payload weight output from FLOPS throughout the mission. As shown in the figure, the CG envelope ranges from 32.99 ft from the nose to 33.18 ft from the nose, corresponding to 32.54% of the MAC and 34.05% of the MAC, both points well forward of the neutral point.
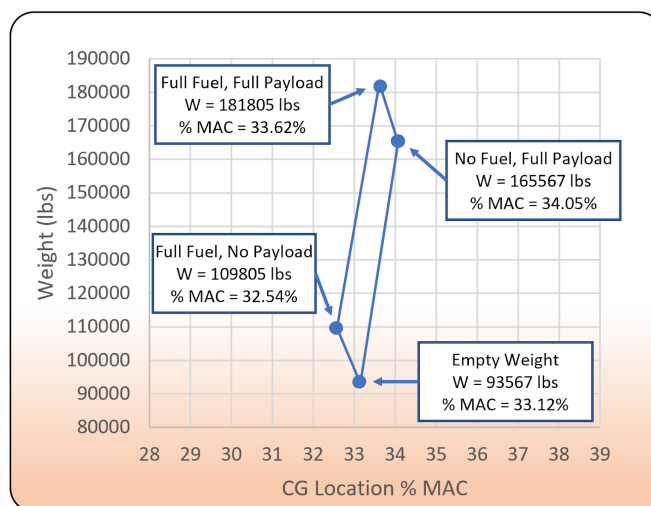
Figure 13-2. CG Travel wrt Wing MAC

14. Auxiliary Systems

The Auxiliary Systems Section covers all of the airplane subsystems: flight controls, engine controls, fuel systems, electrical systems, emergency systems, avionics, camera systems, and anti-icing systems. The Flight and Engine Controls Sections describe the various flight computers and throttle devices used in the aircraft. The Fuel Systems Section reviews the placement of the fuel tanks and describes their connection to the engine. Next, the Electrical Systems Section provides a wiring diagram and reports relevant electrical specifications. The Emergency Systems Section elaborates on subsystems utilized during off-design operation, including one-engine-inoperable and cabin depressurization scenarios. The Avionics Section details the navigation, communication, and autonomy equipment used in the design. Finally, the Targeting and Anti-Icing Systems Sections recount the methods and devices responsible for retardant drop targeting and ice mitigation, respectively. All of the aforementioned sections will leverage off-the-shelf components to ensure an EIS before 2030 and reduce team workload.

14.1 Flight Controls

The Dragonforce's control surfaces are all controlled electronically by a computer system that is centralized in the cockpit. While the plane is sufficiently stable, it uses a fly-by-wire system that allows pilots to easily adapt to the new control scheme. Additionally, the Dragonforce has a manual override system in case of power loss to the computer system. The system is triple-redundant, with two computer systems operating from either side of the cockpit and one computer system located aft of the fire retardant storage tanks. This location for the third computer system was chosen because it allows for a large physical range between the systems in case one part of the Dragonforce is damaged during flight. Furthermore, the access panels that will be used to complete tank maintenance can also be used to access the computer system.

All of the control surfaces are part of the same hydraulic system that controls the landing gear as described in Section 12.4, and each control surface has a complementary actuator attached to the aircraft at the hinge to perform the needed deflections. This includes two ailerons located on the wings' trailing edges on either side of the fuselage, two flaps located inboard of the ailerons, two elevators on either side of the horizontal stabilizer, and a rudder located on the horizontal stabilizer. All of these control surfaces can be deflected at will by the pilot, and the

flaps have preset takeoff and landing settings in which they deflect 25° and 50° respectively. Figure 9-6 depicts the location of the control surfaces.

While the repair and maintenance costs of having three computer systems to maintain the control surfaces will be increased, it was deemed necessary for the aircraft due to the nature of the missions it will complete as it is in dangerous conditions. While a novel computer program is required for the system to control this specific setup of control surfaces, the physical systems and actuators can be adapted from existing aircraft of the same class such as the DC-10 or the C-130.

14.2 Engine Controls

The engine control system will mainly be used to allow the pilot to control the throttle on the dual CFM56-7Bs. The CFM engine class is controlled by the BAE Systems Full Authority Digital Engine Control (FADEC). The FADEC system works by "constantly monitoring and automatically adjusting an aircraft's engine performance and related criteria throughout each flight… [which] allows pilots to focus their energy and attention on the environments they are flying through" (BAE Systems, 2021). The FADEC system provides the pilot with throttle control along with crucial information such as fuel levels, consumption, and engine health.

On engine startup, the pilot of the Dragonforce will turn on the fuel pumps from the cockpit to start the bleeding of fuel from the tanks in the wings into the engines. The pilot can then flip the ignition switch, which will have two settings by standard practice, so the pilot has to switch the position in order for the engine to ignite.The pilot can then use the control dials in the cockpit that tell the appropriate valves in the engine to open, starting at the ground setting then changing based on the flight mission. All of these controls are conducted through the wiring systems that run throughout the aircraft, starting from the cockpit.

Engine stall would only be predicted to occur if the aircraft is operating outside of its appropriate flight envelope. If it were to occur, the pilot is advised to reduce the throttle manually until the stall subsides, and slowly reintroduce the thrust to the engines. Engine malfunction is only predicted to occur in case of damage to the engine during the flight. The engine must be immediately shut down to avoid further damage, and a safe landing area should be found as soon as possible.

14.3 Fuel Systems

To save space in the fuselage, the fuel tanks are located inside the wings. The Dragonforce will employ Integral Fuel Tanks, where the empty space between the wing spars is sealed with a fuel resistant sealant on all sides to prevent leakage. The tank will therefore be formed as a unit within the wing structure itself, giving the aircraft "wet wings". Integral fuel tanks provide the most fuel capacity with the least amount of weight and will be easy to implement since they are used on most modern transport and high performance aircraft (Aeronautics Guide, 2017). The wing spars will serve as built in baffling to prevent sloshing during flight. Check valves will be present on some of the spars to ensure the fuel only flows towards the inner sections of the wing. The fuel pumps to the engine will be located in the inner section of the wing, with fuel boost pumps present in the surrounding baffles to ensure fuel will always reach the engine. These boost pumps can also transport fuel to other tanks to prevent balance issues, along with fueling the aircraft and jettisoning fuel in emergencies. For maintenance purposes, there will be access panels placed along the bottom side of the wing for inspections and repairs. These panels will be sealed with a rubber o-ring and aluminum gasket, with a clamp ring on the inner edge lined with mounting bolts for the access panel.

From FLOPS, the required fuel capacity for the design mission is 16,238 lbs of fuel, including reserves (Table 13-1). Using standard A-1 jet fuel at 6.7 lb per gallon, 2,423 gallons of fuel are required for the design mission. A preliminary volume estimate of the entire section between the outer wing spars yielded a maximum volume of 470 ft^3 per wing and a potential maximum fuel capacity of 3,516 gallons per wing. This is well above the required fuel capacity, as the Dragonforce only needs 324 ft^3 total or 162 ft^3 per wing to meet the 2,423 gallon fuel requirement. Therefore, the fuel tanks will only be located in the four empty spaces closest to the engine to ensure ease of maintenance and decrease the amount of pumps needed.
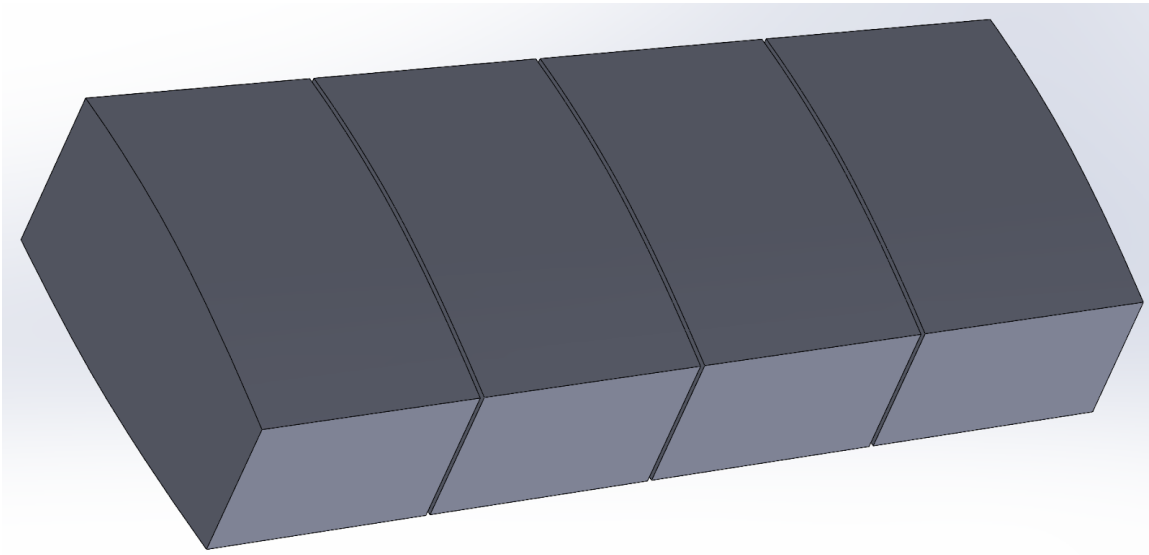
Figure 14-1. Isolated Fuel Tanks

Depicted above are the final isolated fuel tanks, which have a total volume of 195 ft^3 per wing. This final configuration gives the Dragonforce a total fuel capacity of 2,916 gallons, giving the aircraft some extra emergency fuel capacity if necessary. If future design work requires future wing and fuel systems modification, the Dragonforce can be easily adapted.

14.4 Electrical Systems

In order to power the aircraft, two AC generators will reside within the turbofan engines and produce electricity as the turbine turns. This AC current will then pass through a DC rectifier in order to convert to the necessary DC voltage. DC voltage can then charge the main battery system that connects to all necessary electronics. These electronics include the DC powered hydraulics for the control surfaces as well as the main instruments in the cockpit. All other electronics such as the payload dropping mechanism should also be powered by DC.
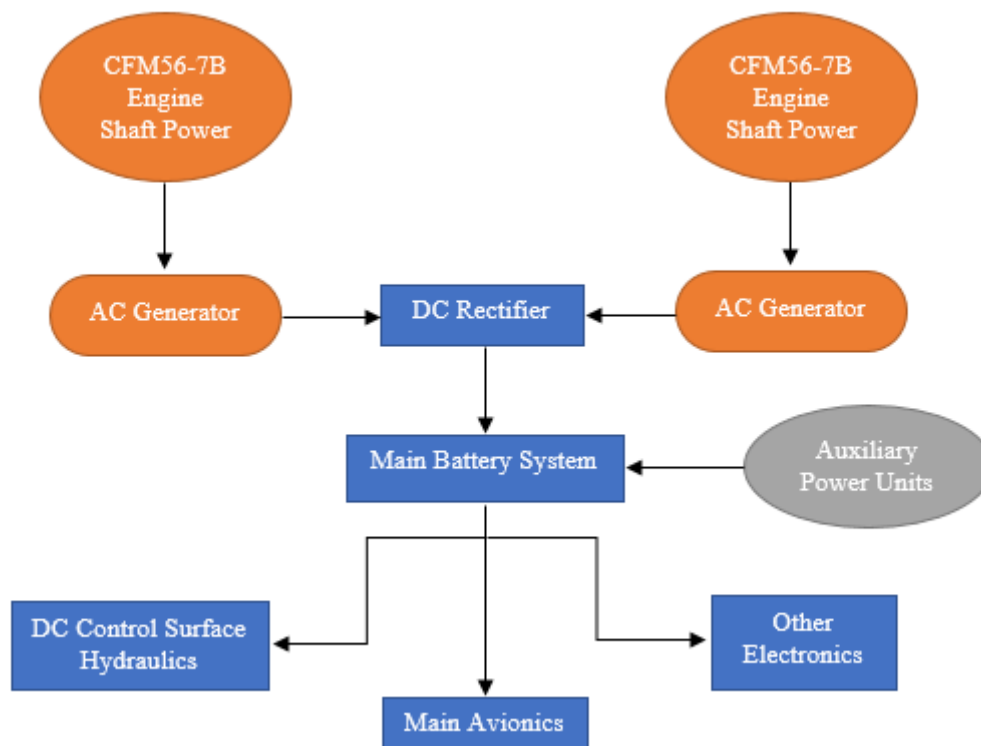
Figure 14-2. Basic Electrical System Diagram

14.5 Emergency Systems

During a rapid response mission, it is crucial to have safety measures in place. With large amounts of smoke, engine performance can be negatively affected. This could even result in engine failure and thus power loss. In the event of an emergency power failure, the Dragonforce is equipped with two independent engines for redundancy. Only one engine and AC generator is necessary to power the main systems; however, in the event both engines fail, the Dragonforce is equipped with an auxiliary power unit (APU). The APU will act as a small turbine engine and power the battery enough for the main instruments and all other necessary electronics to function properly. The APU resides in the tail of the plane and provides no thrust but can be started off the main battery running off bleed air. This also assists with engine relight (SKYbrary Aviation Safety, 2021).

14.6 Avionics

The large-scale avionics systems for the Dragonforce are composed of off-the-shelf systems that are currently used in the C-130. This is done to increase maintainability and repairability of the aircraft, as well as to reduce the training required for pilots. Other smaller systems are pulled from other aircraft in order to increase visibility and improve accuracy while firefighting. It was determined that the Dragonforce would not use an avionics architecture that allows for autonomous operations for multiple reasons. Since the mission is meant to be as accurate as possible while dropping retardant, the team decided that fire recognition by computers would be too difficult to implement in an effective way. Most large air tankers utilize a "lead plane" to direct the drop locations, which leads to an improvement in accuracy. In an attempt to remove the lead plane, the vision capabilities of the pilots must be expanded by the use of camera technology as discussed in Section 14.7. Additionally, one of the largest military drones, Northrupp Grumman's RQ-4 Global Hawk, with a payload capacity of 2,000 lbs, is estimated to cost $131 million (Heath, 2020). If a drone system like this was increased in scale to have a payload capacity of 72,000 lbs for retardant, then the cost would be significantly increased and completely infeasible. For those reasons, it was decided that the Dragonforce will be a piloted aircraft similar to that of existing state-of-the-art large air tankers used in aerial firefighting. The avionics architecture for the Dragonforce will be that of the C-130H systems aside from the following systems:

- **Radar:** The Dragonforce will utilize the AN/APQ-122 radar system developed by Raytheon (Cloer, 2020). This system will allow mission success in various weather conditions like smoke, fog, and darkness. The dual-frequency radar system will provide pilots with additional visuals in order to improve flight safety and drop accuracy by enabling ground mapping for terrain avoidance and long-range navigation. The main components of the system include antenna, electronic control amplifier, receiver/transmitter, and radar stabilization control.

- **Communications:** Raytheon's MXF-626K VHF radio system will be installed in the Dragonforce in order to have an optimal communications system providing UHF, VHF, AM, and FM transmissions. These systems also allow the plane to meet the new European air traffic control requirements in the event of European leasing (Katam, 2015) . The MXF-626K provides the Dragonforce with air-to-air and air-to-ground communication which will help in coordination of drop locations and accuracy.

- **FLIR:** Forward-looking infrared (FLIR) systems allow pilots to visualize heat signatures in their surroundings, which would allow visibility of fires to increase while dropping retardant. FLIR technology uses infrared radiation to develop either video or images that can then be displayed to pilots on a heads up display (HUD) or superimposed on the visor of a helmet the pilot is wearing (Krapels & Driggers, 2004). With smoke put off by forest fires, FLIR systems will allow pilots to see through the obstruction and locate fires. FLIR systems can also extend the mission time allowing pilots to operate later in the evening or early in the morning.

14.7 Camera Systems

As part of a possible advanced concepts initiative, the design has the capabilities to support a camera and radar system, with the goal of transmitting live wildfire data to a publicly developed, easily accessible database. The camera setup as part of the underside of the fuselage will contain two main parts—a camera and a mount. For the camera, we have chosen the Raytheon MTS-A, and for the mount, we have chosen the Trine Aerospace and Defense Retractable Camera Mount System.

MTS sensors provide detailed intelligence data from the visual and infrared spectra in the form of high definition full motion video. It is the hope of the group that this video can be utilized in a separate system to produce data on the wildfire location, speed, and predicted path. Specifically, this camera utilizes a combination of electro-optical/infrared (EO/IR), laser designation, and laser illumination capabilities all in one. Due to the higher resolution, EO/IR camera ball systems are very effective tools for providing overwatch for specific areas of interest on a wildland fire, detecting spot fires or new fires, providing support for ground operations, monitoring impingements of trigger points, and identifying location and amount of residual heat during the mop-up phase.

As for the Trine Retractable Camera Mount System, the standard system kit includes a retractable camera mount, wire harness, control circuit, bayonet mount, RCMS Installation/Operations manual, optional manual retract system, and an optional deployment door system. The camera weighs 60 pounds, and the mount weighs 39 pounds, for a total additional cargo weight of 99 pounds to the final design. The total volume of the mounted camera system will be 4.06 cubic feet. We are confident the design has sufficient volumetric margin in our fuselage, so the added volume was not considered during testing.

The main benefit of adding a system such as this to our design is to have the capability to better inform regulators, operators, and the public of possible dangers in the event of a wildfire. Keeping an affected population up to date with live images and data regarding a natural disaster is valuable, and we believe it will lead to the community being better prepared to face a wildfire head on. Due to the relatively small added weight, we are confident the impact to acquisition, fly away, and direct operating costs will be negligible, especially in light of the significant utility offered by the addition of this subsystem.

14.8 Anti-Icing Systems

For modern aircraft, anti-icing systems are essential to prevent ice build-up and subsequent flow separation around the airfoil. Currently, anti-icing methods can be classified into three categories: (1) the liquid-based, such as weeping wings; (2) the mechanical-based, such as pneumatic boots; and (3) thermal-based, such as hot-air and electro-thermal systems. After considering all three options, the team decided to use commercially available electro-thermal anti-icing systems because they are widely used on comparator aircraft (Meng et al., 2019). Furthermore, the wing will be coated with an ice-phobic coating such as NANOMYTE SuperAi (NEI, 2021).

14.9 Retardant Refueling Systems

In order to meet the RFP requirement for fire retardant reload greater than 500 gallons per minute, it is necessary to specify the equipment at the ground station for refilling the payload tanks. A Waterous CXS high flow rate split-shaft pump, as shown in Figure 14-5 was selected and configured to properly interface with the payload tank. The pump has a maximum flow rate of 1,500 gal/min, and with a single pump for each tank, the retardant can be reloaded in just over 2.5 minutes. Weighing 228 lbs, the pump can easily be installed on tanker vehicles at the ground station so that the aircraft can be reloaded on the runway to minimize turnaround times. The pump is configured to interface with the payload tanks via a dry disconnect coupling, which provides an automatic mechanism to seal off both the hose and the fixed pipe end when the hose is disconnected. This prevents any leakage of the corrosive retardant in the fuselage interior.
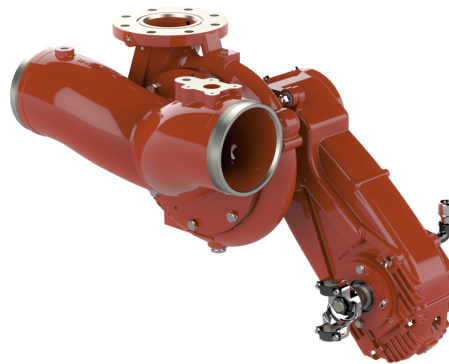
Figure 14-3. Water CSX High Flow Rate Split-Shaft Pump

15. Maintenance

While maintenance might not be commonly discussed in the conceptual design process, it is arguably just as important as any other design feature. It is critical to ensure that the aircraft is designed so that maintenance can be completed cost effectively and without undue burden to the operators. This section will discuss three main areas that are expected to receive maintenance throughout the aircraft's life cycle: the airframe, engine, and retardant tanks.

15.1 Airframe Maintenance

Aerial firefighting is an atypical environment that poses increased risks to the airframe. The low altitude payload drops will expose the Dragonforce to high temperatures, low visibility, airborne debris, and irregular air currents. Combined, these factors ensure the aircraft's airframe will be more stressed than ordinary transport aircraft.

Beyond routine airframe maintenance that all transport aircraft undergo, there are a few unique concerns for maintenance presented by aerial firefighting. Debris impact can occur when the aircraft flies too close to the tree canopy or when debris is blown upwards from unexpected updrafts. The aircraft's exterior must be regularly inspected for any abnormalities present in the skin. Regular airworthiness standards will be used to determine whether the aircraft can remain in service or should be serviced.

Furthermore, fire retardant will accelerate corrosion on the aluminum surfaces (FAA, 1995). This will be significantly mitigated by using carbon fiber reinforced polymers for the fuselage skin, but there will inevitably be some exposure to the aluminum frame. Therefore, the corrosion maintenance cycle must be shortened to ensure airframe integrity. Finally, the multiple pull up and descent maneuvers performed during each mission will stress the wings more than usual for similarly sized transport aircraft. Regular inspections of internal fuselage and wing structures will most likely be performed at a slightly more frequent rate to limit or fix crack propagation.

15.2 Engine Maintenance

Along with the concerns mentioned in the previous section, the primary concern regarding engine maintenance is foreign object debris (FOD) ingestion, which can severely damage internal engine components and possibly result in total system failure. In fact, tree branches up to 18 inches in length can become airborne from strong wind gusts (Colorado State Forest Service, 2012). Furthermore, the air entering the engines will likely be

contaminated with ash and other particulates. Both of these factors shorten the engine service life and maintenance cycles. While the shortened service life increases cost, the increased cost is inevitable in these types of environments. With that being said, the Dragonforce uses off-the-shelf-engines that are placed on pylons for easy removal and maintenance. Moreover, the CFM56-7B engines are known for their reliability, with a 99.96% dispatch reliability rate (Levingston, 2019).

15.3 Retardant Tank Maintenance

Due to the corrosive nature of fire retardant mixtures, the metallic lower hopper and fire gates must be coated with a corrosion preventive compound before each flight season. This maintenance is facilitated by the removable design of the upper polyethylene tank portion. Additionally, if any issue arises during inspection, the upper portion of the tank can be disconnected and replaced with a new one in a short timeframe. The choice of polyethylene for the upper tank not only reduced weight but also negated the requirement for coating of the tank interior, which is difficult to access. In addition to the repair and maintenance of the tank structure itself, special care must be taken to inspect and service the hydraulic firegate doors. This includes routine inspection and lubrication of the operating linkages that are housed below the fuselage floor. Finally, at the end of each flight cycle, the retardant tanks should be rinsed to remove any residual retardant. This can be done at the ground station by pumping the tanks full of water and completely emptying them.

16. Cost Analysis

The Cost Analysis Section covers all costs associated with production, operation, and payload. For production costs, material costs and labor hours are estimated using the DAPCA IV and Raymer models. These models do not include inflation rates, so those are considered separately. The Operating Costs Section involves operating, repair, and fueling costs for an aircraft. The Cost of Payload Section discusses the cost associated with the chosen payload for the Dragonforce design mission. Every mission will have at least 4,000 gal of flame retardant, which can be expensive to mix in large quantities. The overall cost was modeled using AAA.

16.1 Production Cost

For the production costs, it was assumed that the plane would be modeled after a military transport rather than a commercial transport aircraft. This simplified the necessary inputs for AAA in the research, development, test, and evaluation (RDT&E), and acquisition phases of production. Only one test plane should be needed for this stage in order to reduce costs. For the final design, several assumptions were made based on the Roskam method of cost estimation. For the RDT&E phase, the velocity was assumed to be 314 KEAS based on a cruising mach of 0.6. The Difficulty Factor was set to 1.0, as this is a fairly conventional aircraft design. Similarly, the CAD judgment factor is set to 0.8 as the design team is experienced with CAD. The observability factor has been set to 1.0 as no stealth capabilities are required for this plane. The avionics and materials cost factors have been set to 0.5 and 1.0, respectively. This was assumed because the avionics system is moderately complex for the dropping system, and the body of the plane consists of mostly conventional aluminum alloys. Finally, the manufacturing, tooling, and engineering rates from 1989 come directly from Roskam and are $32, $44, and $61 per hour respectively.

In addition to the parameters above, the entry into service year, 2030, was chosen for the cost estimates. This came with a cost escalation factor of 7.67. The weight of the plane as well as the number and type of engines seemed to have the largest effect on the production costs. Table 16-1 below summarizes all of the costs associated with the total RDT&E and acquisition costs for the Dragonforce.

<p style="text-align:center">**Table 16-1.** Summary of Production Costs for the Dragonforce</p>

|	
Total RDT&E Cost	$968.6 Mil
Total Manufacturing Cost	$2.32 Bil
Total Acquisition Cost	$2.32 Bil
TOGW	181,800 lbs
Engine Number and Type	2 Turbofan

16.2 Operating Cost

Operational costs for military aircraft can be broken down into 7 major factors: direct personnel, indirect personnel, materials, fuel and lubricants, spares, depot, and miscellaneous costs. Personnel costs, direct and indirect, are tied to the cost of the crew operating and maintaining the aircraft. Materials costs are associated with consumable materials used for aircraft maintenance. Fuel and lubricants costs are for fuel and any other lubricants or oils used for the aircraft. Spares and Depot costs are associated with spare parts and overall maintenance costs. All other costs fall under the miscellaneous costs. The operational costs for this aircraft would be nearly entirely direct operating costs due to it being modeled as a military aircraft. Per the RFP, annual hours were assumed to be 1,200 hours. The average mission block time was assumed to be 6 hours (worst case scenario, assuming only ferry missions) along with 15 years operational life. For the crew, it was assumed only 3 people would be needed for a mission: pilot, co-pilot, and an engineer to monitor the tanks. Based on Roskam's data, the pay for these crew members was assumed to be $59,000 per year.

The total operating cost for the final design is $580.96 million at approximately $4,000 per hour. Looking at a comparable aircraft, the C-130's operating cost per hour is around $7,000 per hour. Thus, the Dragonforce is significantly cheaper than comparator aircraft. The maximum capacity of the final design is more than double the capacity of the C-130 at nearly half the cost. Figure 16-1 shows the breakdown of the total operating cost.
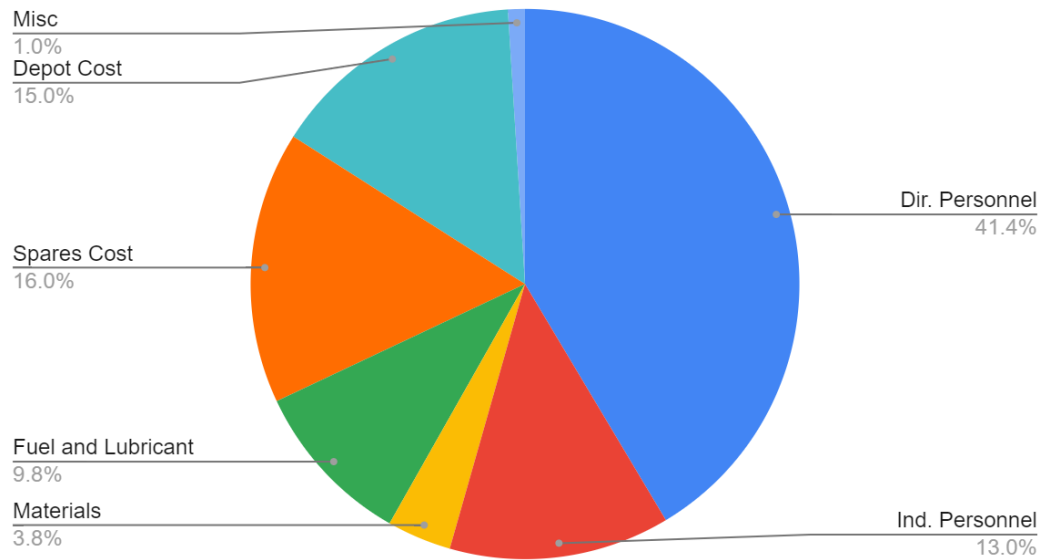
Figure 16-1. Final Operating Cost Breakdown

16.3 Flyaway Cost

Flyaway cost can be seen as the cost to produce a single unit after the original production has been completed. For cost estimation, it was assumed that 10 units would be produced originally and all acquisition costs are for the entire line, not individual aircraft. Table 16-2 summarizes the total acquisition and flyaway costs for the final design.

Table 16-2. Total Acquisition and Flyaway Costs for the Dragonforce

Total Acquisition Cost	$2.32 Bil
Individual Unit Cost	$232.40 Mil
Flyaway Cost	$200.08 Mil

16.4 Cost of Payload

In an interview with The Sun, Cal Fire Deputy Director Janet Upton is quoted saying, "Phos-Chek, the red fire retardant used during wildfire, brings a cost of $2.50 to $3.50 per gallon" (Saunders, D., 2017). With this value, it can be estimated that the payload cost can range from $20,000 to $28,000 for 8,000 gallons of payload. As this was reported in 2017, inflation should be accounted for. With a price increase of roughly 17% since 2017, the cost of the payload in 2022 would be $23,400 to $32,760.

16.5 Overall Cost

The overall cost or life cycle cost (LCC) is the total cost of all stages of production and operation of an aircraft plus a disposal cost. Disposal cost is calculated based on a disposal factor multiplied by the sum of all other total costs. The disposal factor was set to 0.01 as 1% would be reasonable for shorter, rapid response missions. A summary of total costs from all stages of the program and the LCC can be found in Table 16-3.

Table 16-3. Life Cycle Cost for the Dragonforce

Total RDT&E Cost	$968.63 Mil
Total Operating Cost	$580.96 Mil
Total Acquisition Cost	$2.32 Bil
Disposal Cost	$39.13 Mil
LCC	$3.91 Bil

17. Conclusion

The importance of aerial firefighting has continuously expanded as global warming and desertification have proliferated worldwide. The purpose of this report was to describe the iterative process that the team went through to design a conceptual next generation aerial firefighting aircraft. Large air tankers provide a pivotal role in the system of aerial firefighting and can be considerably improved from existing retrofitted aircraft systems. For this reason, the RFP asked for the design of an affordable aerial firefighting aircraft (AIAA, 2021). As shown throughout the report, the Dragonforce is a highly effective and capable next generation aerial firefighting large air tanker. It meets all of the requirements and many of the objectives outlined by the RFP.

The payload capacity of 8,000 gallons maximized the objective for payload size, allowing for large amounts of fire retardant to be dropped, covering a large land area, and effectively cutting off wildfires from additional fuel. With the Dragonforce's ability to meet all of the objectives for range, radius, dash speed, and drop speed, the conceptual design is the definition of specialized next generation aerial firefighting aircraft. The Dragonforce will be able to remain on extended missions and increase the volume of retardant dropped on a fire per day—significantly negating the strength of wildfires. Additionally, modeling the Dragonforce off of the preexisting C-130 will allow for quicker time-to-repair and reliability compared to significantly modified designs. With an acquisition cost of $232.4 million per unit for a total of 10 units built, the resulting flyaway cost after this original line has been completed would be approximately $200 million. The Dragonforce is a feasible option in the aerial firefighting market with an operational cost just over $4,000/hour, which is much lower than comparable retrofitted military systems that are currently in use. The Dragonforce exceeds the RFP's specifications and is an affordable specialized aircraft that represents a compelling new product helping to solve firefighting challenges.

In the future, the Dragonforce concept could be further developed into a tangible product. While outside the scope of this report, the team has shown that the design meets many RFP objectives and has a niche in the current aerial firefighting market. Furthermore, future analysts could repeat the analysis in this report with higher fidelity tools to increase accuracy and validate the underlying assumptions in the lower fidelity models.

Figure 17-1. Rendered Image of The Dragonforce Dropping Retardant

References

Aeronautics Guide. (2017, June). Types of aircraft fuel tanks. Aeronautics Guide.

https://www.aircraftsystemstech.com/2017/06/types-of-aircraft-fuel-tanks.html

AIAA (2021). American Institute of Aeronautics and Astronautics. Request for proposal - responsive aerial

firefighting aircraft.

Allied Market Research. (2021). *Firefighting Aircraft Market to Reach $16.46 Billion, Globally, by 2030 at 6.5%*

CAGR: Allied Market Research. Cision PR Newswire.

https://www.prnewswire.com/news-releases/firefighting-aircraft-market-to-reach-16-46-billion-globally-by

-2030-at-6-5-cagr-allied-market-research-301425240.html

Asmatulu, R. (2012). Nanocoatings for corrosion protection of aerospace alloys. *Corrosion Protection and Control*

Using Nanomaterials, 357–374. https://doi.org/10.1533/9780857095800.2.357

BAE Systems. (2021). *FADEC: The Brains behind the Brawn Optimizing the World's Aircraft Engines.* Commercial

Aircraft Solutions. https://www.baesystems-ps.com/fadec.php.

Balle, J. (2020). *CFM International CFM56 (F108).* PowerWeb.

http://www.fi-powerweb.com/Engine/CFM56-F108.html

Behera, A., & Mallick, P. (2020). Application of nanofibers in the aerospace industry. *Fiber-Reinforced*

Nanocomposites: Fundamentals and Applications, 449–457.

https://doi.org/10.1016/b978-0-12-819904-6.00020-7

Blaesser, N. (2020). *Interference Drag Due to Engine Nacelle Location for a Single-Aisle, Transonic Aircraft*

[Doctoral thesis, Virginia Polytechnic Institute and State University]. VTechWorks.

http://hdl.handle.net/10919/96446

Brady, C. (1999). *CFM 56-3 Specific Operating Instructions.* The 737 Information Site.

http://www.b737.org.uk/cfm56_soi.htm

CFM. (2018). *CFM 56 Overview.* CFM Aero Engines.

https://www.cfmaeroengines.com/wp-content/uploads/2019/12/Brochure_CFM56_2018.pdf

Cloer, L. (2020, June 3). *AN/APQ-122 - the C-130 hercules' eyes while in the Sky*. Duotech Services. Retrieved May

2, 2022, from https://duotechservices.com/apq-122-c130-hercules-eyes-sky

Colorado State Forest Service. (2012). *Protecting Your Home from Wildfire: Creating Wildfire-Defensible Zones.*

   https://static.colostate.edu/client-files/csfs/pdfs/FIRE2012_1_DspaceQuickGuide.pdf

EASA. (2019). *Type-Certificate Data Sheet for V2500-A5, V2500-D5, V2500-E5 Series Engines.*

   https://www.easa.europa.eu/sites/default/files/dfu/IM%20E%20069%20Issue04_20191212.pdf

EASA. (2021). *Type-Certificate Data Sheet for RB211 Trent 500 Series Engines.*

   https://www.easa.europa.eu/downloads/7701/en

FAA. (1995). *Corrosion of Aluminum Alloys in the Presence of Fire-Retardant Aircraft Interior Materials.*

   http://www.tc.faa.gov/its/worldpac/techrpt/ar9581.pdf

Goodyear. (2018). *Global Aviation Tires.* https://www.goodyearaviation.com/resources/pdf/databook-6-2018.pdf

Hall, D. K., Huang, A. C., Uranga, A., Greitzer, E. M., Drela, M., & Sato, S. (2017). Boundary Layer Ingestion

   Propulsion Benefit for Transport Aircraft. *Journal of Propulsion and Power*, *33*(5), 1118–1129.

   https://doi.org/10.2514/1.b36321

Heath, H. (2020, June 10). *How much does the RQ-4 Global Hawk cost?* Rampfesthudson.com. Retrieved May 2,

   2022, from https://www.rampfesthudson.com/how-much-does-the-rq-4-global-hawk-cost/

Helan, A. (2022). *How increased threat of forest fires and climate change in Southeast Asia is further endangering*

   public health. South China Morning Post.

   https://www.scmp.com/comment/opinion/asia/article/3169306/how-increased-threat-forest-fires-and-climat

   e-change-southeast

Inagak, I., Shirai, Y., Takechi, T., & Ariyasu, N. (2014). Application and Features of Titanium for the Aerospace

   Industry. *NIPPON STEEL & SUMITOMO METAL TECHNICAL REPORT*, 22–27.

   https://www.nipponsteel.com/en/tech/report/nssmc/pdf/106-05.pdf

Jeevanantham, V., Vadivelu, P., & Manigandan, P. (2017). Material Based Structural Analysis of a Typical Landing

   Gear. *International Journal of Innovative Science, Engineering & Technology*, *4*(5), 295–300.

   https://ijiset.com/vol4/v4s4/IJISET_V4_I04_34.pdf

Katam, P. (2015, December 11). *Raytheon to equip US C-130H Hercules aircraft with Advanced Radio Systems*.

   Airforce Technology. Retrieved May 2, 2022, from

https://www.airforce-technology.com/news/newsraytheon-to-equip-us-c-130h-hercules-aircraft-with-advanced-radio-systems-4751391/

Krapels, K., & Driggers, R. G. (2004). Imaging: Infrared Imaging. Encyclopedia of Modern Optics, Five-Volume Set, 152–163. https://doi.org/10.1016/B0-12-369395-0/00709-0

Levingston, C. (2019). *1 Billion Flight Hours: "World-class experience" builds 15,000th CFM56-7B engine*. GE Aviation Blog.

https://blog.geaviation.com/manufacturing/1-billion-flight-hours-world-class-experience-builds-15000th-cfm56-7b-engine/#:~:text=The%20CFM56%20engine%20is%20known,or%20cancellation%20every%202%2C500%20departures

Martins, D. (2015). *Off-Design Performance Prediction of the CFM56-3 Aircraft Engine.* Instituto Superior Técnico.

https://fenix.tecnico.ulisboa.pt/downloadFile/1126518382177922/DanielMartins_ExtendedAbstract.pdf

Meng, X., Hu, H., Li, C., Abbasi, A. A., Cai, J., & Hu, H. (2019). Mechanism study of coupled aerodynamic and thermal effects using plasma actuation for anti-icing. *Physics of Fluids*, *31*(3), 037103.

https://doi.org/10.1063/1.5086884

Modern Airliners. (2022). *Airbus A320 Specs – What is behind one of the most popular short-haul airliners?*

https://modernairliners.com/airbus-a320-introduction/airbus-a320-specs/

NASA. (2020). *Flight Optimization System (FLOPS) Software, V.9.*

https://software.nasa.gov/software/LAR-18934-1

NEI. (2021). *The Development of NEI's Anti-Ice Coating Technology for the Aerospace Industry.*

https://www.neicorporation.com/anti-ice-for-aerospace-case-study/

Nicolai, L. M., and Carichner G. E. Fundamentals of Aircraft and Airship Design, Vol 1, AIAA Education Series, Virginia, 2010.

Raymer, D. P. (1999) *Aircraft Design: A Conceptual Approach*. American Institute of Aeronautics and Astronautics.

Romano, A. (2022, April 14). *Here's why planes fly at 36,000 feet*. Travel + Leisure. Retrieved May 2, 2022, from

https://www.travelandleisure.com/airlines-airports/why-do-planes-fly-at-36000-feet-cruising-altitude#:~:text=According%20to%20USA%20Today%2C%20the,36%2C000%20feet%20in%20the%20air.

Roskam, J. (1985). *Airplane Design.* Roskam Aviation and Engineering Corporation.

Saunders, D., & Rokos, B. (2017, September 6). *Massive - and pricey - 747 joins Cal Fire's arsenal to battle wildfires*. San Bernardino Sun. Retrieved May 4, 2022, from https://www.sbsun.com/2017/09/02/cal-fires-new-firefighting-aircraft-is-pricey-but-worth-it-officials-say/#:~:text=Phoschek%2C%20the%20red%20fire%20retardant,%243.50%20per%20gallon%2C%20Upton%20said

Schaufele. R.D. (2007). *Elements of Aircraft Preliminary Design*. Aries Publications.

SKYbrary Aviation Safety. (2021, May 26). *Auxiliary Power Unit (APU)*. Retrieved May 4, 2022, from https://skybrary.aero/articles/auxiliary-power-unit-apu#:~:text=An%20Auxiliary%20Power%20Unit%20or,high%20pressure%20air%20start%20cart

Waterous. (2017). *CXK/CXPA | Fire Pumps, Fire Supplies*. Waterous Fire Pumps & Protection Equipment. https://www.waterousco.com/cxk-ckpa.html